DETERMINATION OF

OCULAR THRESHOLD LEVELS FOR

INFRARED RADIATION CATARACTOGENESIS

Donald G. Pitts, O.D., Ph.D.
Anthony P. Cullen, O.D., M.Sc.
Pierrette Dayhaw-Barker, Ph.D.
University of Houston
College of Optometry
Houston, Texas 77004

NIOSH # 77-0042-7701

U.S. DEPARTMENT OF HEALTH AND HUMAN SERVICES
Public Health Service
Center for Disease Control
National Institute for Occupational Safety and Health
Division of Biomedical and Behavioral Science
Cincinnati, Ohio 45226

JUNE 1980

For sale by the Superintendent of Documents, U.S. Government
Printing Office, Washington, D.C. 20402

DISCLAIMER

The contents of this report are reproduced herein as received from the contractor. The opinions, findings, and conclusions expressed herein are not necessarily those of the National Institute for Occupational Safety and Health, nor does mention of company names or products constitute endorsement by the National Institute for Occupational Safety and Health.

NIOSH Project Officer: C. Eugene Moss
Principal Investigators: Donald G. Pitts, O.D., Ph.D.
Anthony P. Cullen, O.D., Ph.D.

ACKNOWLEDGMENTS

The authors wish to express appreciation to Karsten Neilsen, O.D., for assistance in all of the primate research and the latter stages of the rabbit studies.

DHHS (NIOSH) Publication No. 80–121

ABSTRACT

A 5000 watt Xenon high pressure lamp was used to expose 100 pigmented rabbit eyes and 10 monkey eyes to both infrared radiation and the full optical spectrum of the source. The primary ocular lesion was an anterior epithelial sub-capsular opacity which initially was seen as small whitish dots that developed into white patches in that area of the anterior capsule just beneath and in contact with the iris. No lenticular opacities were induced by direct exposure to the lens. Ocular damage from infrared exposure was related to the rate of delivery of the radiation. Infrared irradiances up to 3.9 $W \cdot cm^{-2}$ resulted in thresholds for the rabbit eye of 5000 $J \cdot cm^{-2}$ for the cornea, 3500 $J \cdot cm^{-2}$ for the iris, and 3750 $J \cdot cm^{-2}$ for the lens while irradiances above 4.0 $W \cdot cm^{-2}$ gave rabbit ocular thresholds of 1250 $J \cdot cm^{-2}$ for the cornea, 1250 $J \cdot cm^{-2}$ for the iris, and 2250 $J \cdot cm^{-2}$ for the lens. Exposures with the full optical spectrum of the source showed that the visible and the ultraviolet radiation were additive for damage to the lens. The monkey ocular thresholds were a factor of 6 above the respective rabbit threshold. The methodology for ocular protection, the criteria for ocular damage, and the levels of allowable infrared exposure are discussed.

CONTENTS

INTRODUCTION

Purpose of the Research

The purpose of the research was to establish the ocular threshold exposure values for infrared radiation (IR) in the 700 to 1400 nanometers (nm) wavelength range necessary to produce cataracts in the crystalline lenses of experimental animals relevant to man, to identify and report effects observed in other ocular structures, and to recommend valid criteria for safety standards against ocular exposure to IR.

Review of the Literature

An extensive review of the literature was not necessary because of the papers of Turner (1), and Duke-Elder (2) and the exhaustive review by Moss et al. (3). Therefore, this section covers selected research, which produced experimental data, in an attempt to acquaint the reader with the irradiance levels in the IR spectrum necessary to produce ocular damage or to confirm that such data do not exist.

An understanding of the absorptive or transmittance properties of the eye in the wavelength region of concern will assist in explaining some of the observed biological effects. Weisinger et al. (4), Geeraets et al. (5), Boettner and Wolter (6), Prince (7), and Geeraets and Berry (8) have published transmittance data for the rabbit, primate and human in the wavelength range from 300 nm to 2000 nm (Figures 1-3). These reports indicate that the mammalian ocular media are transparent to the near IR (radiation in the 750 nm to 1400 nm wavelength range) and essentially opaque to the far IR (radiation greater than 1400 nm). The corneal transmittance exceeds 90% between 500 and 1300 nm. Beyond 1300 nm, absorption bands at about 1430 nm and 1950 nm are found for the cornea but its transmittance remains high between these bands. Beyond 2000 nm, the IR absorption of the cornea appears to be almost complete. The aqueous humor transmits to about 2400 nm and has absorption bands centered at 980, 1200, 1430 and 1950 nm. The crystalline lens shows high transmittance to about 1400 nm with absorption bands centered at 980, 1200, and 1430 nm. The transmittance of the vitreous humor exceeds 90% and demonstrates absorption bands at 980 nm and 1200 nm with essentially no transmittance of IR beyond 1400 nm.

Thus, IR above 2000 nm is absorbed almost entirely by the cornea and aqueous humor. Almost all of the near IR impinging on the iris is absorbed by the iris pigment epithelium layer which lies next to the lens. The near IR which passes through the pupil shows strong absorption bands above 900 nm while almost none of the IR above 1400 nm reaches the retina. The IR which is transmitted through the ocular media to the retina is absorbed by the pigment epithelium of the retina.

The ocular effects of IR on the different anatomical structures beginning with the eyelid and proceeding posteriorly to the retina will be reviewed.

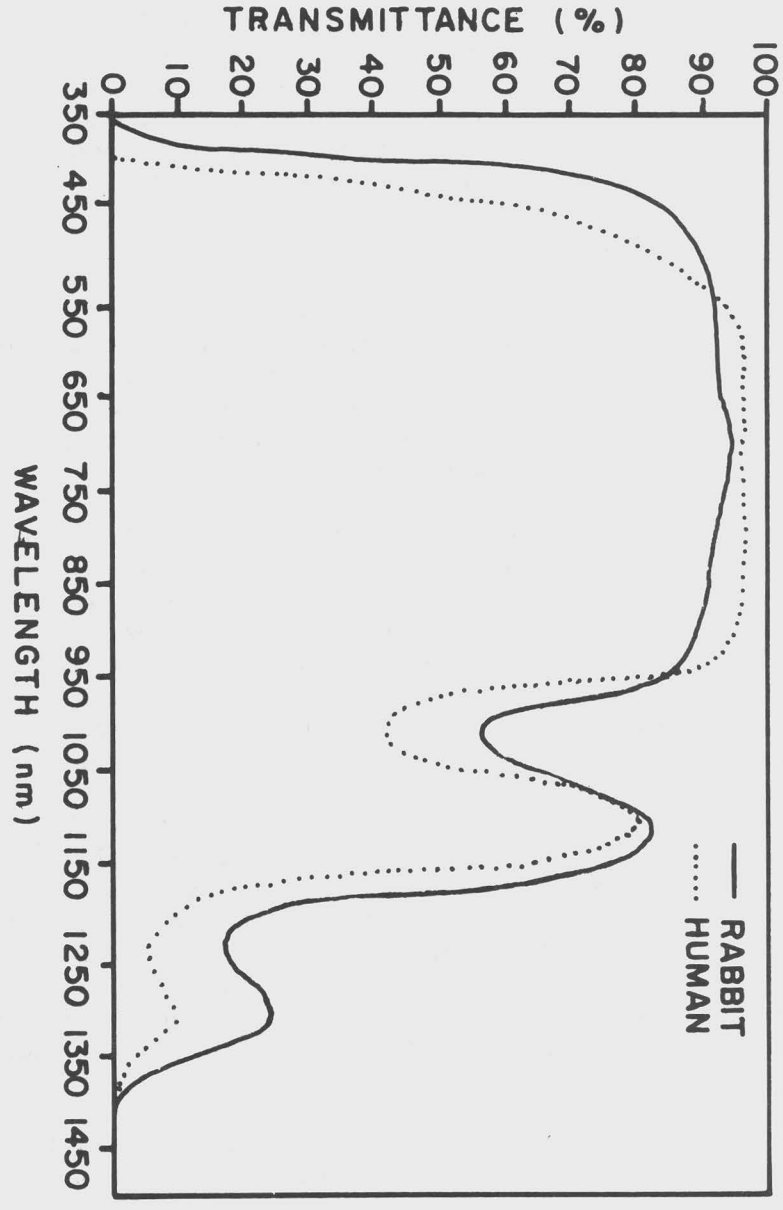

Figure 1. Transmittance curves for the human and rabbit ocular media (after Geereats).[5]

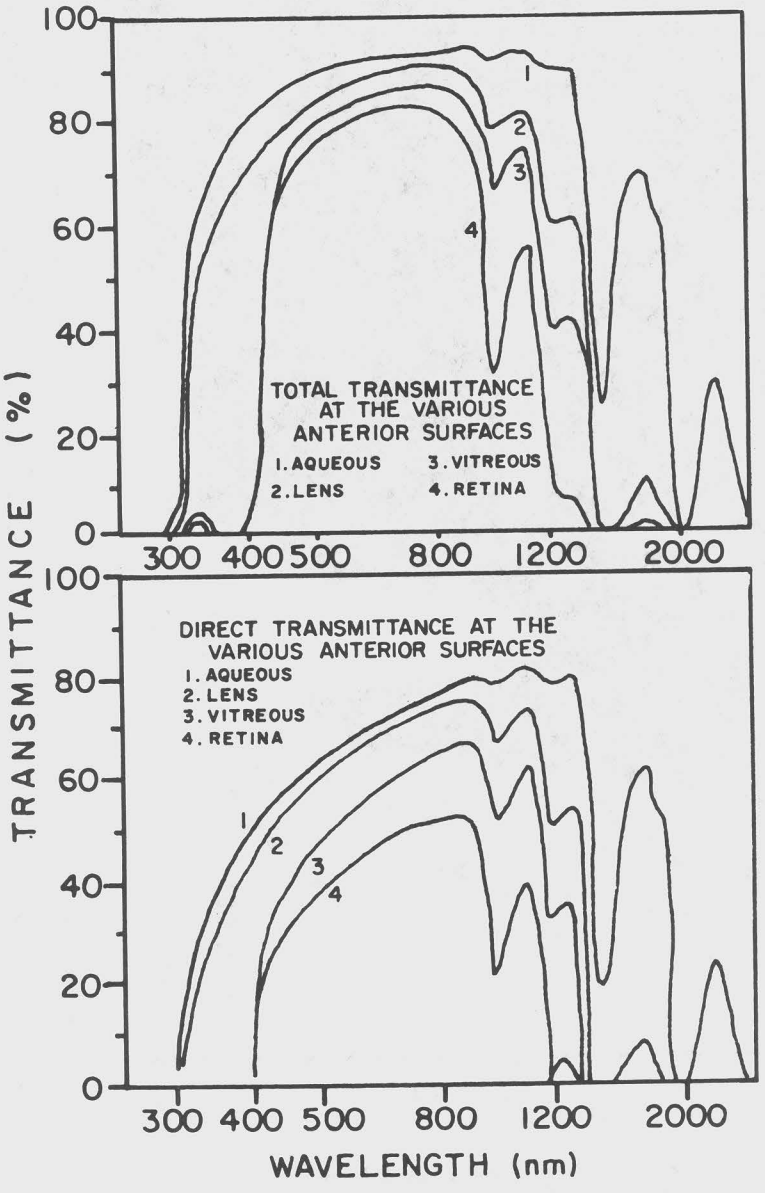

Figure 2. Total and direct transmittance of the components of the human eye (after Boettner and Wolter).[6]

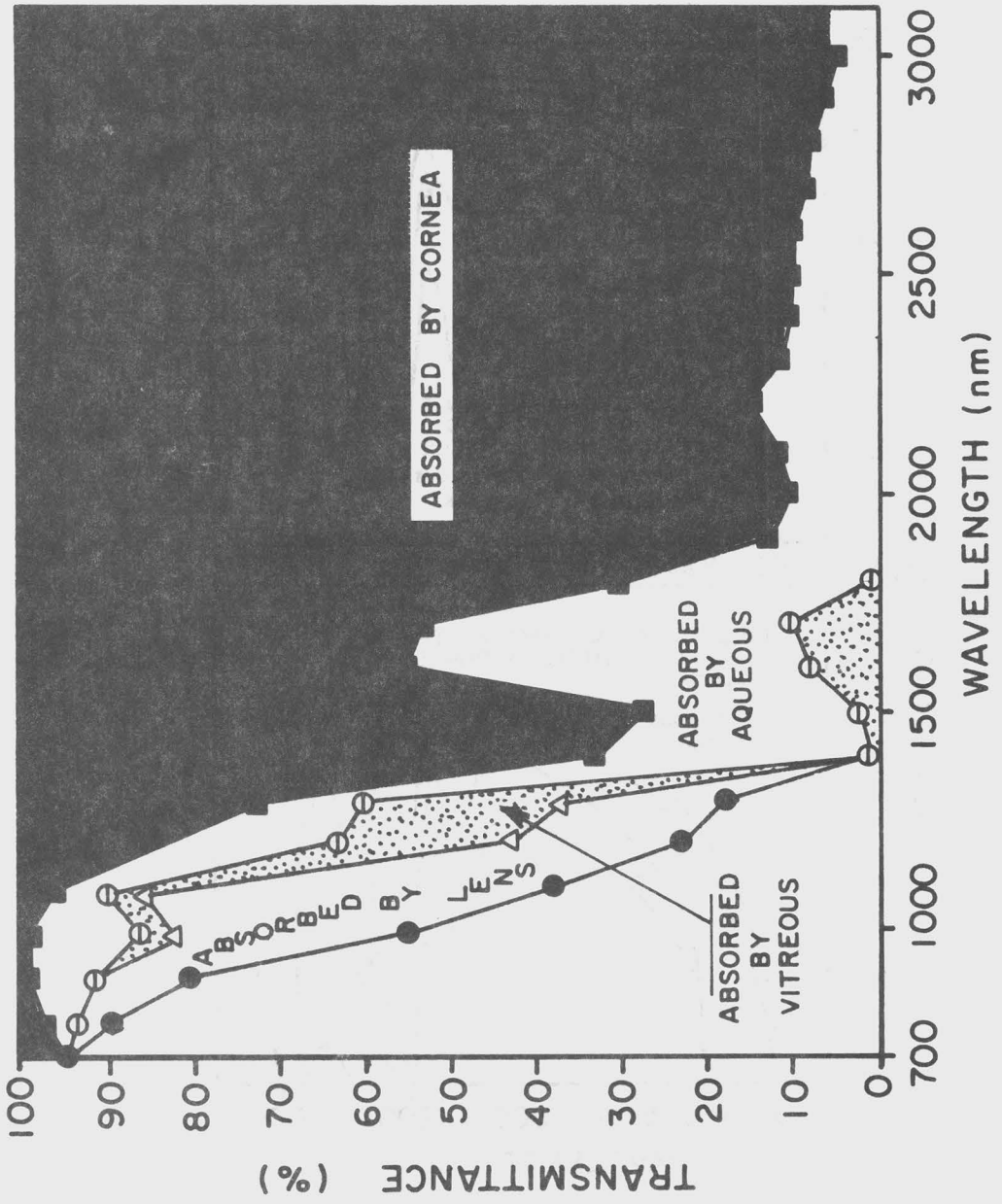

Figure 3. Composite of the absorption of infrared by the ocular components (after Kutscher).[25]

Eyelids

The effects of IR on the eyelids range from erythema to third degree burns and necrosis of the skin (2). To obtain these effects, the eyelid must be exposed to very high levels of IR delivered over a short period of time or exposed to low to moderate levels of IR over a long period of time. IR eyelid damage is not ordinarily experienced in the industrial environment.

Cornea

IR effects on the cornea consist essentially of protein coagulation of the epithelium and the stroma; however, the drying of the cornea and reflex closure of the lids occur prior to any coagulation (5). Verhoeff and Bell (9) emphasize that the posterior layers of the cornea may demonstrate more damage than the anterior layers because the lacrimal fluid and the air cooling of the anterior layers of the cornea are more effective than the aqueous cooling of the posterior layers of the cornea by convection. The coagulation of corneal tissues results in immediate pain, reflex closure of the eyelids, and protective movements of the head and eye.

Dawson (10) used a Sylvania DFA tungsten filament lamp with a parabolic reflector to expose the left corneas of 26 cats. The spectral output of the lamp was not measured, but Dawson reported its wavelength range as 400 nm to 2600 nm with a total radiant emittance at 150 W of 7.04 $g \cdot cal \cdot sec^{-1} \cdot cm^{-2}$ (29.5 $J \cdot cm^{-2}$). Exposure durations were from 15 s to 365 s. The exposed eyes were examined by slit-lamp with changes in the cornea ranging from mild to ulcerating lesions while cataract formation was seen in the lenses. Dawson summarized the results as follows:

Total Dose	Ocular Effect
100 $g \cdot cal \cdot cm^{-2}$ (418.5)* $J \cdot cm^{-2}$	No immediate effect 24 hours - mild leukoma 72 hours - complete recovery
100 $g \cdot cal \cdot cm^{-2}$ to 300 $g \cdot cal \cdot cm^{-2}$ (418.5 to 1255.5)* $J \cdot cm^{-2}$	Corneal opacities Corneal vascularization Penetrating ulcers
300 $g \cdot cal \cdot cm^{-2}$ (1255.5)* $J \cdot cm^{-2}$	Deep penetrating corneal ulcers

*4.185 $J \cdot cm^{-2}$ per $g \cdot cal \cdot cm^{-2}$ was used for conversion

It should be remembered that certain tungsten lamps produce a spectrum in the ultraviolet (UV) beginning at about 250 nm and some of the effects described above parallel closely the description of those produced by UV exposures.

Iris

Duke-Elder (2) has summarized the effects of IR on the iris. He stated that even moderate doses of IR result in an aqueous flare, hyperemia, and miosis. Severe exposures may result in a paralytic mydriasis, congestion with hemorrhages, thrombosis, and stromal inflammation. These effects result in necrosis of the iris with bleached, atrophic areas forming within a few days. In addition, there is a loss of pigment at the edge of the iris within two to four days after exposure. Unfortunately, the radiant exposure levels were not quantified.

Crystalline Lens

The first mention of the effects of IR on the crystalline lens was in 1739 (1). Many authors pointed out the relationship between certain types of cataracts and occupations which required prolonged exposure to heat. Meyenhofer (11) was the first to study glassworkers and to provide data on the number of workers who developed cataracts. He described the posterior cortical opacity which has become accepted as the early stages of the IR-induced cataract. In 1907, Legge (12, 13) was instrumental in establishing the glassblowers cataract as a legal occupational disease. Robinson (14) argued that the IR was the cause of the "heat cataract."

Vogt (15, 16) used a carbon arc lamp (4000 K) filtered through water and iodine sulphate to expose rabbit eyes. The principal effects reported were to the cornea, iris, and lens. Vogt maintained that the cataract was due to direct absorption of the IR by the lens. The results reported by Vogt could have been the result of UV exposure since the carbon arc source was rich in UV and filtered by water.

Verhoeff and Bell (9) are noted for their research on the effects of UV; however, their research extended to the IR spectrum, using a low pressure quartz lamp, the magnetite arc, and the sun. The lower limit of the spectrum was controlled by crown and flint ophthalmic glass filters. When the lower spectrum was limited to 305 nm, the lens was damaged, but if the spectrum was limited at 295 nm, the endothelium, iris, and lens were damaged. They filtered sunlight with a 2 mm thickness of UV101 glass and used a large mirror to focus the transmitted energy to the iris and the pupil of the pigmented rabbit eye. Exposure durations were 15 seconds and 30 seconds with the animal's eye placed at 1.0 meter from the mirror. The anterior lens epithelium of the pupil was unaffected but the lens epithelium beneath the pupil and in contact with the iris pigment epithelium demonstrated a "mitosis similar to observations produced in other experiments by abiotic (UV) radiations." In other words, that portion of the lens covered by, and in contact with, the iris showed lenticular opacities but no response was found in that portion of the lens seen through the pupil. They argued that the cataract was due to interference with normal ciliary body function and the subsequent interference with lens metabolism.

Goldmann (17-24) exposed rabbit eyes to a specially designed furnace source. He measured ocular transmittance of IR and experimentally induced cataracts in the crystalline lens in that portion of the lens under the iris. Goldmann was not able to produce cataracts by direct exposure of the lens through the pupil. Goldmann claimed that IR or heat cataracts were not due to direct absorption of the IR by the lens but due to the raising of the temperature indirectly through heat absorbed by the iris.

From the 1930s to date there were many reviews of the literature, very few epidemiological studies, and a few experimental studies which provided data on which some conclusions could be reached. Kutscher (25) reviewed the literature on "glassblower's cataract" and concluded that it was in the third decade of life that puddlers, tin platers, and steel rollers appeared to develop cataracts. He also reviewed the Vogt-Goldmann controversy for the cause of cataracts without arriving at a conclusion. Salit (26) discussed the rise in incidence in cataracts one year after a very dry, hot summer in Iowa together with data reports from the weather bureau. He concluded that more attention should be paid toward environmental conditions as causative agents for cataracts. Dunn (27) reviewed the causes of industrial cataracts in workers at the Corning Glass Works. He concluded that the cataracts were not caused by IR but by other etiological factors. He calculated the irradiance at eye level from glass manufacturers to be 2.0 $g \cdot cal \cdot cm^{-2} \cdot min^{-1}$ or 0.139 $W \cdot cm^{-2}$. Keatinge et al. (28) surveyed the incidence of lenticular changes in an iron rolling mill. Of 44 workers examined only 3 (6.8%) of the workers, all over 65 years of age, showed the "classical posterior cortical lenticular changes" described as typical of heat or IR cataracts. They calculated the radiation at the rolling mill to be from 0.08 $W \cdot s^{-1} \cdot cm^{-2}$ to 0.42 $W \cdot s^{-1} \cdot cm^{-2}$. The control group showed 16 posterior capsular opacities (15%), of which 7 were in workers under 50 years of age. The authors state that cataracts occur in the general population at equal or greater levels of incidence than in iron rolling mill workers, but that certain individuals may be more susceptible to radiation cataracts than others. Hence, the workers and control individuals who developed cataracts may simply have been susceptible individuals.

Wallace et al. (29) examined 1000 steel workers, 100 of whom were not at risk and 900 of whom were exposed to low, intermediate, and high levels of IR. The workers were scored on the infrared exposure levels as 3 for a high exposure, 2 for intermediate, 1 for low, and 0 for no exposure. They classified cataracts according to type: Type I were small lenticular disturbances which did not interfere with vision; Type II were posterior subcapsular saucer-shaped opacities causing minimal interference with vision; and Type III were dense posterior subcapsular opacities which produced gross disturbances in vision. An exposure index was calculated by multiplying the number of years on the job by the exposure risk. The exposure index was compared to the type cataract which was found. No Type III cataracts were found. The percentage of Type I cataracts increased with age from about 50% at the age of 40 to about 62% at the age of 65. They found only two exposed workers with cataracts which were attributed to their occupation; however, a slightly higher incidence of the common cataract due to aging was found in the groups exposed to IR.

Langley et al. (30) repeated the experiments of Goldmann and hypothesized that both visible light and IR must be absorbed by the iris for cataracts to be produced. Six groups of 5 rabbits were each exposed to a 100 W zirconium arc lamp with a focused image of 6.75 mm^2, an irradiance of 0.154 $W \cdot cm^{-2}$, for 30 s which gave a radiant exposure of 4.62 $J \cdot cm^{-2}$. The exposure beam was directed to the iris. The animals were sacrificed at 30, 60, 90, 120, and 150 days after irradiation. The clinical sequence was a burn-like thickening and clouding of the cornea, an anterior uveitis, and a disruption of the iris followed by iris pits or holes if the radiant exposure was high. Within 2 to 3 weeks, the lens developed a whitish area which changed to a grayish opacity below the anterior capsule. By 6 weeks, the lenticular opacity extended toward the equator and joined with a cup-shaped posterior sub-capsular opacity to form a U-shaped cataract. The opacity remained unchanged at this stage or progressed to encompass the whole crystalline lens. Langley et al. stated that if the iris were exposed midway between the pupillary margin and the root of the iris, a cataract could be produced in almost every eye. They argued that it was not the total heat applied to the eye, but the increase in the temperature at a local area which produces the cataract.

Most of the experimental evidence appears to support the theory of Goldmann; however, there are speculations which still question this view. For example, the excessive number of "solar cataracts" found in India could be due to UV and/or nutrition. Not all workers in the metal industry develop cataracts; and, many studies attempting to support Goldmann's theory used sources which contained UV which was apparently not filtered out. Nevertheless, most of the opinion is strongly in favor of the Goldmann hypothesis. It is also interesting to note that most researchers found posterior lenticular cataracts induced by IR only after a long latency of 30 to 90 days. In contrast the IR cataracts described in some research were described as anterior subcapsular opacities with the posterior sub-capsular and equatorial involvement being found only after long latencies. Pitts and Cullen (31) have recently reported that 100% of the pigmented rabbits used in experiments demonstrated a posterior subcapsular lenticular opacity which radiated laterally along the horizontal posterior suture line, in some rabbits almost to the equator, and occasionally projected anteriorly from the posterior suture line at the posterior pole of the lens into the cortex and into the nucleus of the lens. The density and proliferation of these opacities increases normally with age. The findings suggest that long term effects which have been reported in the literature may be nothing more than the normal aging process of the rabbit.

Retina and Choroid

The primary effect of IR on the retina and the choroid is increased temperature. It is beyond the scope of this study to review all of the data in the literature relative to retinal lesions from photic stimulation. This is especially so since most research in retinal burn lesions employed

broad band spectral sources which usually included some UV, the visible, and the IR spectra. Hence, it is difficult to separate from each other the effects of different regions of the spectrum. Therefore, a few reports have been selected from which IR damage data may be evaluated.

The experimental variables in producing retinal lesions include pupil size, spectral transmittance of the ocular media, spectral absorbance of the retina and choroid, the optical quality of the retinal image, exposure duration, size of the source, location on the retina, size of the retinal image, the type of source, spectral distribution of the source, rate of delivery of the energy, and the criteria used to evaluate the exposures. Exposure duration is an important parameter even if all other parameters are held constant. As the exposure duration increases, the radiant power entering the eye necessary to produce a retinal lesion decreases until duration becomes ineffective and a lesion appears to be determined by the irradiance reaching the retina.

Bredemeyer et al. (32) used an air-cooled mercury lamp for the UV and short visible radiation, a high-pressure Xenon lamp for a continuous wavelength spectrum from 250 to 1300 nm, and a carbon arc system which provided a 250 nm to 5000 nm continuous spectrum to study the effects of narrow spectral wavelength exposures on the eye. They exposed adult pigmented rabbits to six wavebands while maintaining constant retinal image size and exposure durations. Their data showed that the longer wavelength radiation required higher irradiances at the cornea to produce a retinal burn.

Jacobson et al. (33) exposed adult chinchilla rabbits to the visible and near IR region of the spectrum. They used a Zeiss photocoagulator with a 1600 W Xenon lamp source and varied the rate of delivery, the retinal image size, the exposure duration, and the spectral characteristics of the source. Their data for LD-50 and spectral characteristics are summarized as follows:

Ocular Structure	Wavelength in nm	Corneal Dose in $cal \cdot cm^{-2}$	Corneal Dose in $J \cdot cm^{-2}$
Cornea:	370-480	0.70	2.93
	480-590	0.75	3.14
	620-1100	1.20	5.02
	870-1120	1.90	7.95
	1200-1670	0.70	2.93

Iris: 0.3 to 0.5 $cal \cdot cm^{-2}$ (1.25 $J \cdot cm^{-2}$ to 2.09 $J \cdot cm^{-2}$) produced a minimal irreversible lesion. Iris exposures given below are measured at plane of the cornea.

Wavelength in nm	Corneal Dose in $J \cdot cm^{-2}$	Corneal Dose in $cal \cdot cm^{-2}$	Corrected Corneal Dose in $J \cdot cm^{-2}$	Corrected Corneal Dose in $cal \cdot cm^{-2}$
370-480	3.97	0.95	1.63	0.39
480-590	3.26	0.78	1.72	0.41
620-830	3.35	0.80	2.13	0.51
880-1120	11.29	2.70	4.89	1.17

Lens: 9.21 to 10.05 cal·cm^{-2} (38.53 to 42.05 J·cm^{-2}) measured at the plane of the cornea resulted in no visible lesion to the lens. There was no filter used during this exposure phase.

370-900 nm - radiant exposure of 2.4 to 4.59 cal·cm^{-2} (10.0 to 19.21 J·cm^{-2}) resulted in no visible lesion to the lens.

880-1120 nm - radiant exposure of 1.77 to 1.88 cal·cm^{-2} (7.41 to 7.87 J·cm^{-2}) resulted in no visible lesion to the lens.

The data of Jacobson et al. indicate that ocular damage can occur to the iris with radiant corneal exposures as low as 0.39 J·cm^{-2} and to the lens with more than 42.05 J·cm^{-2}.

Ham et al. (34) recently reported that to produce retinal lesions of 159 μm in size in the rhesus monkey radiant exposures on the retina from two spectral wavebands, 400 to 800 nm and 700 to 1400 nm, were required with exposure durations of 1, 10, 100, and 1000 seconds. They found reciprocity was maintained for exposures to the 400 to 800 nm waveband for exposure durations 10 s or longer with the radiant exposure being 400 J·cm^{-2}. A radiant exposure of 6.91 x 10^{4} J·cm^{-2} was required for the 1000 s exposure using the near IR of 700 to 1400 nm wavelength range. They were unable to produce a retinal burn with exposure durations less than 1000 s.

Levels of Exposure to Workers

Barthelmess and Borneff (35) measured the total daily radiation received by glassblowers working near the melting furnaces and found the total radiation to be 2000 to 3000 J·cm^{-2}. Approximately 10% of that total was IR below 1400 nm. Sliney and Freasier (36) stated that the IR corneal dose rate from daylight is about 10^{-3} W·cm^{-2}. They report that glass and steel workers exposed to IR irradiances on the order of 0.04-0.08 W·cm^{-2} daily for 10-15 years develop lenticular cataracts. IR corneal irradiances of 0.1 W·cm^{-2} are often used as a guideline for protection against far IR lasers. Sliney and Freasier suggest that the chronic exposure criterion for IR in the 780 to 1400 nm wavelength range should be on the order of 0.01 W·cm^{-2}. Moss et al. (3) provide an excellent tabular summary of industrial IR sources which may provide a hazard to the eye.

INSTRUMENTATION AND PROCEDURES

Infrared Source

The source for the infrared energy was a 5 kW Xenon high pressure lamp, powered by a 10 kW, DC power supply regulated to 0.5% and capable of delivering from 1 to 80 amperes at 25 to 65 volts to the lamp electrodes (Figure 4). The lamp housing was cooled by two air blowers and continuous flow water through copper tubing. The air in the laboratory was conditioned and humidity controlled to with $\pm$ 10%. The 5 kW Xenon source provided a continuous spectrum from 200 nm to 5000 nm with approximately 45% in the IR region.

The radiation from the source was focused at the entrance slit of a McPherson Model 2501, single grating monochromator. The monochromator grating had a wavelength range of 185 nm to 10.4 μ, was blazed at 1200 nm, had 150 lines/mm with a linear dispersion of 6.6 nm per mm of exit slit, and allowed a total band pass of 66 nm while providing an accuracy of 0.05 nm. The monochromator optical system was aligned and the wavelength counter calibrated with a HeNe laser. Stray light was greater than 20% in the IR region of the spectrum; therefore, a Schott RG-715 filter blocking filter was placed in the optical system just beyond the exit slit of the monochromator (Figure 4). The Schott RG-715 filter reduced stray light to an unmeasurable level. The transmittance characteristics of the Schott RG-715 filter were measured with a Beckman Mark VI spectrophotometer and are given in Figure 5.

In addition to using the monochromator as a wavelength device, the grating was positioned at zero wavelength counter reading to allow the central image to pass through the system without undergoing diffraction. The central image contained the full spectrum of the source but could be controlled for exposure durations and filtered to produce the desired wavebands for exposure. When filtered with the Schott RG-715 filter, the spectrum reaching the lens had a wavelength range of 715 nm to 1400 nm because the longer IR was absorbed by the cornea and the aqueous (Figures 3 and 5).

Exposure durations were controlled with an Hewlett Packard Model 5330B preset counter which operated a Gerbands electronic shutter. The shutter system allowed exposure durations of any desired length with millisecond accuracy.

The size of the optical beam at the plane of the cornea could be reduced in size by placing the two lenses in the optical system just beyond the filter. When the lenses were omitted from the optical system, the beam exiting the monochromator was essentially collimated and measured 1.5 cm x 2.5 cm at the plane of the exposure. An exposure made under these conditions was called an "unfocused beam" and covered essentially the entire cornea. With the lenses in the optical system, the beam measured 0.8 cm x 1.5 cm at the plane of the exposure and was called a "focused beam." The focused beam provided

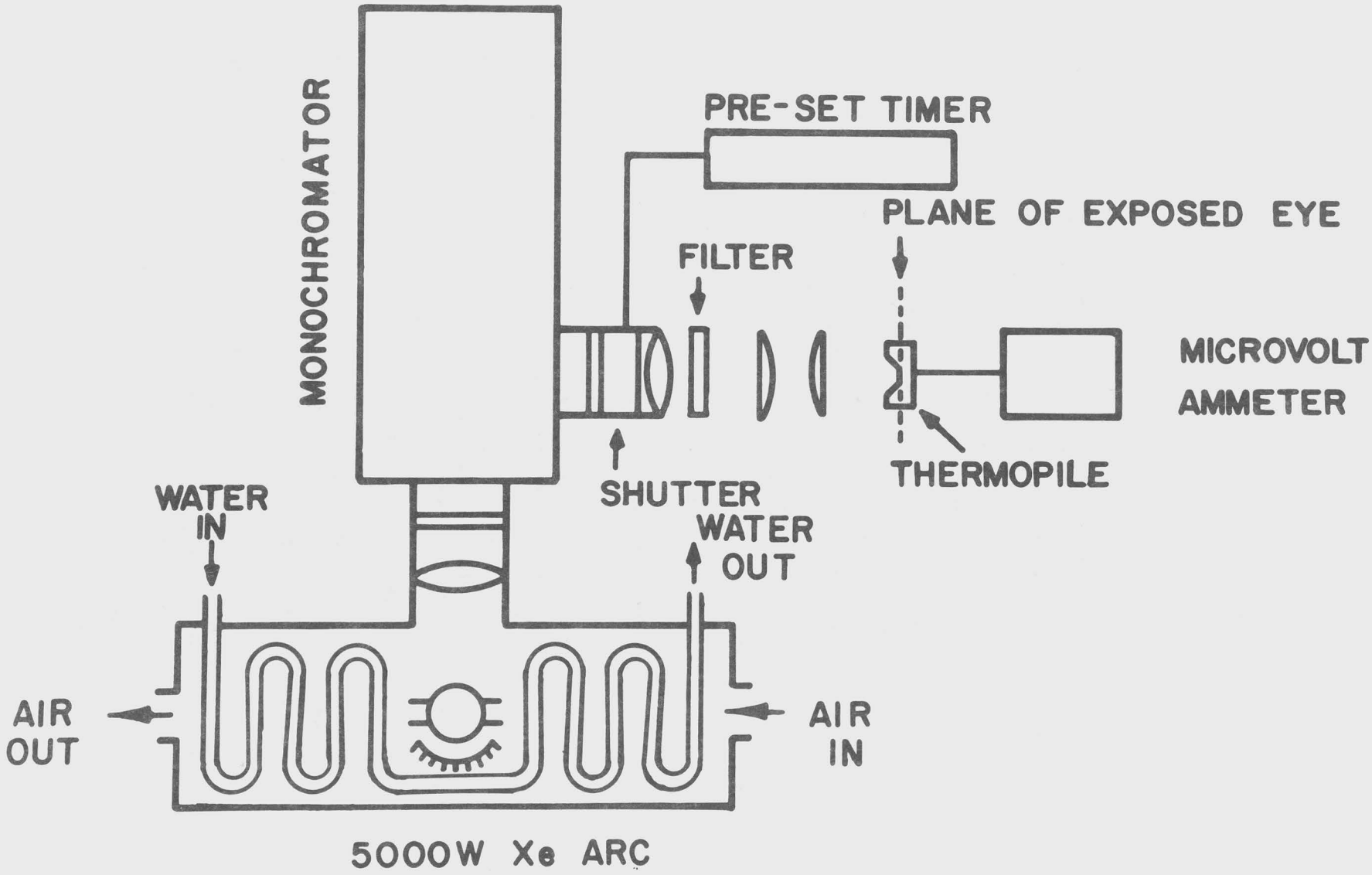

Figure 4. Schematic of the exposure instrumentation. See text for details of description of the system, source measurement, and exposure procedures.

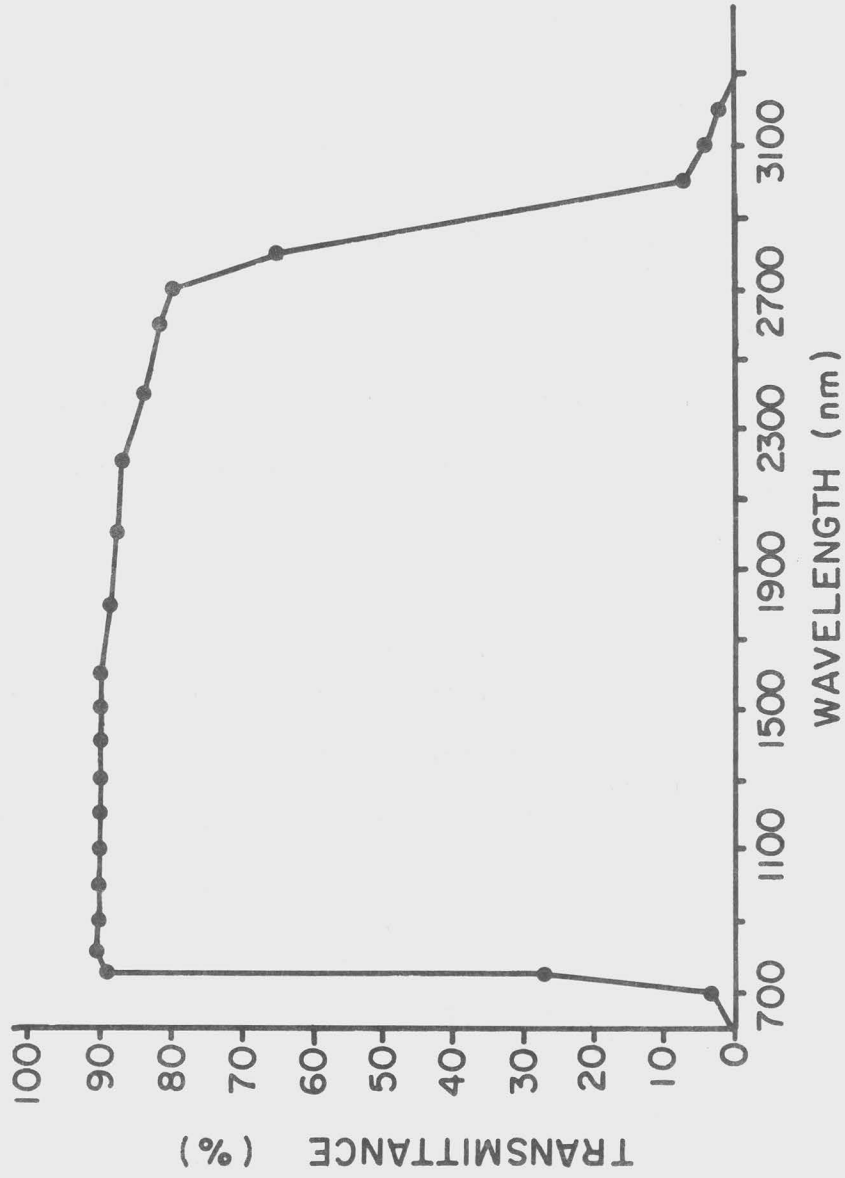

Figure 5. . Spectral transmittance of the Schott RG-715 filter.

two advantages. First, the radiant energy was concentrated into a smaller area increasing the irradiance and, second, the vertical rectangular beam could be directed to expose only the lens (with a dilated pupil), only the iris, or both the lens and the iris simultaneously. The flexibility allowed by the focused beam proved helpful during the course of the research, but eye movements with the focused beam resulted in greater variability in the threshold exposure data than that when the unfocused beam was used. The beam profile was essentially flat throughout its extent.

A special device was constructed and incorporated into the optical system to insure the proper alignment of the animal's eye with the optical beam (Figure 6). The device consisted of two "L" shaped tungsten source filaments which were aligned precisely with the central optical axis of the monochromator optics and were optically focused at the correct distance for exposure. When the animal was placed at the proper distance and aligned with the optical axis for exposure, the "L" filaments formed a cross or "+." A slight lateral or longitudinal misplacement resulted in the loss of the cross of "+" image as illustrated in Figure 6 for longitudinal displacement. The alignment device was used for the initial alignment of the animal's eye for exposure and periodically throughout the experiment to check on alignment.

Infrared Source Measurement

The IR source was measured with an Eppley 16-junction thermopile traceable to an NBS standard source. The thermopile was located in the same position that the animal's cornea would occupy during exposures. The readout amplifier was a Keitheley 150 B microvoltmeter. The irradiance incident on the thermopile was determined by the following formula:

$$E = K \cdot V_T \qquad (1)$$

where E is the irradiance in $W \cdot cm^{-2}$, K the thermopile calibration constant in $W \cdot cm^{-2} \cdot mV^{-1}$, and V_T the thermopile voltage in mV. Equation (1) is valid for the measurement of the irradiance of sources with a diameter equal to or larger than the aperture of the radiometer. To use the thermopile to measure source sizes smaller than the area of the thermopile detector surface, the irradiance formula must be corrected as shown below for the area effects:

$$E = K \cdot V_T \cdot \left(\frac{A_D}{A_B} \right) \qquad (2)$$

In equation (2) A_D is the area of the thermopile detector surface and A_B is the beam area of radiation striking the detector.

The radiant exposure (H) in $J \cdot cm^{-2}$ was calculated by use of the equation:

$$H = E \cdot t \qquad (3)$$

where H is the radiant exposure in $J \cdot cm^{-2}$ and t is the exposure duration in seconds.

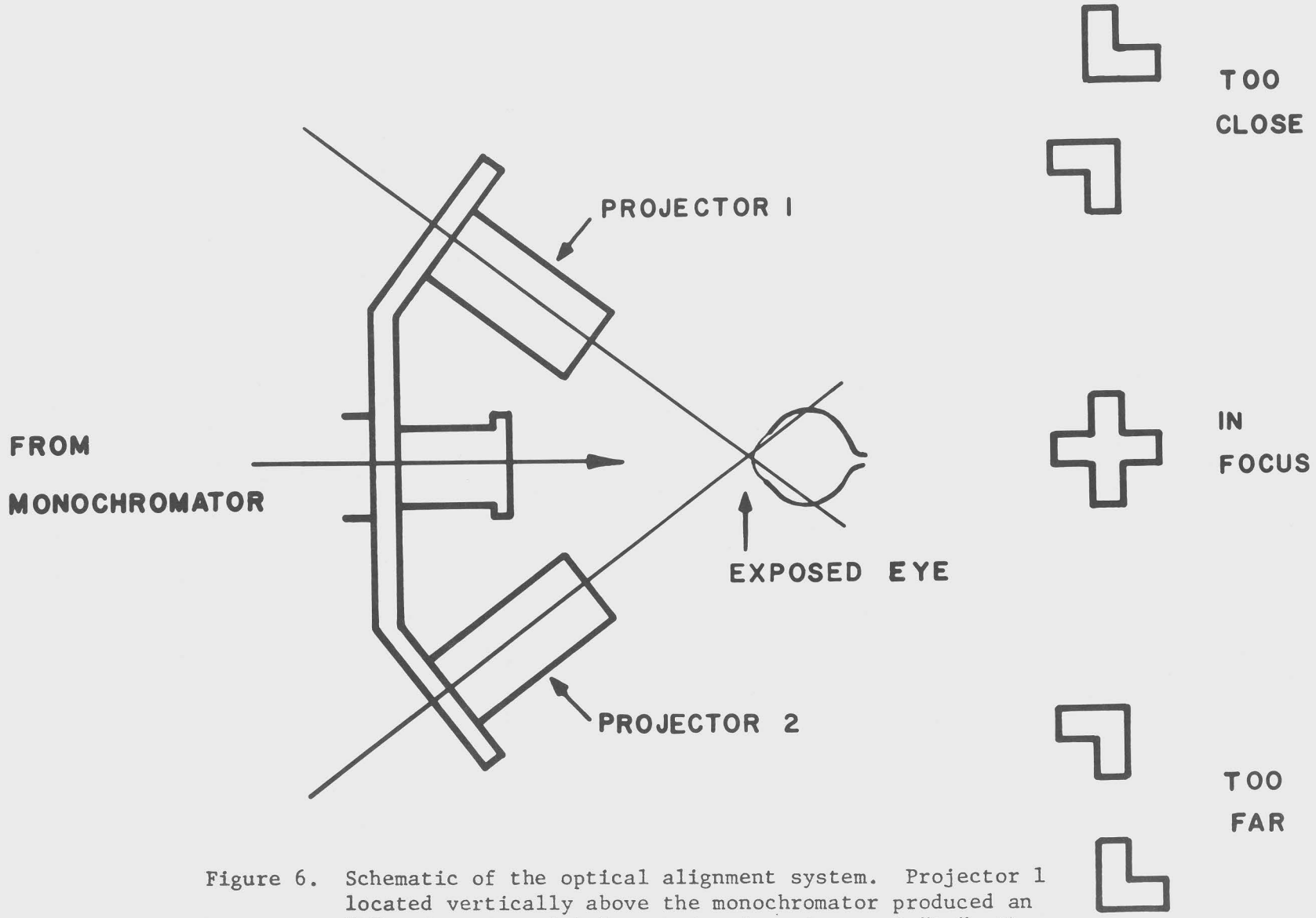

Figure 6. Schematic of the optical alignment system. Projector 1 located vertically above the monochromator produced an "L" and project 2 below produced an inverted "L." The projectors were aligned to produce a "+" on the corneal apex when the eye was aligned laterally, vertically, and longitudinally from the monochromator.

Thus, the source can be measured in irradiance or radiant power units and the exposure duration t varied to obtain different values for the radiant exposure H. The exposure duration t, irradiance E, and radiant exposure H were determined for each exposure using the above procedures. It was estimated that the measurement accuracy of the source was approximately $\pm$ 15%. Figure 7 presents an example of the relative spectral irradiance of the 5 kW Xenon source measured at 50 nm wavelength intervals up to 2100 nm through the RG-715 filter. The spectral irradiance of the source was less than 1.5×10^{-4} $W \cdot cm^{-2}$ for 50 nm waveband intervals up to 3500 nm.

Experimental Animals*

Healthy adult cynomolgous monkesy (Macaca fasciculais), 6.6 to 8.0 kg in weight, and pigmented rabbits, 2 to 3 kg in weight, were the animals used during experimentation without regard to sex.

Since research on UV, visible, and IR effects on ocular structures has been primarily with the rabbit, continuation of the IR research with the rabbit would allow better comparison of the different radiation damage research. The anatomy of the rabbit eye is well known and the differences from the human eye are well established. The rabbit is small, easily handled, and can be examined readily with the biomicroscope and ophthalmoscope.

The cyanomolgous monkey was used because its eye, although smaller than the human eye, more closely approximates the human eye. Therefore, the monkey exposures allow better validation of any proposed protection criteria document.

Exposure Procedures

The experimental protocol was initially intended to determine the action spectrum for IR in 50 nm bandwidths over the 700 to 1400 nm wavelength range. Preliminary exposures using 50 nm waveband at 1050 nm with 1.48 mW irradiance showed that exposure durations up to 13,480 s or 20 $J \cdot cm^{-2}$ did not result in ocular damage. Care was taken to perform all exposures under as normal a physiological condition as possible; however, the preliminary exposures indicated that anesthesia was necessary to prevent discomfort to the animal since the pupil constricted and the nictitating membrane began to move over the cornea within 40 minutes after the exposure began. A second part of the experimental protocol was to test the hypotheses of Goldmann and of Vogt on the development of cataracts from exposure to IR.

In these experiments, the IR spectrum was the output of the source that was transmitted through the RG-715 filter. The full spectrum output included the UV, visible, and IR spectra. The exposure durations were given within a 15 minute to 8 hour time range. These durations were defined in an attempt to limit the laboratory exposures to durations equivalent to the use of sources in industrial processes and to simulate the normal working day for humans.

---

* The care of the experimental animals used or intended for use in the performance of this research complies with "The Guide for the Care and Use of Laboratory Animals," Institute of Laboratory Resources, National Academy of Sciences - National Research Council (HEW Publication (NIH) 73-23) and "The Principles for Use of Laboratory Animals," Department of Health, Education and Welfare.

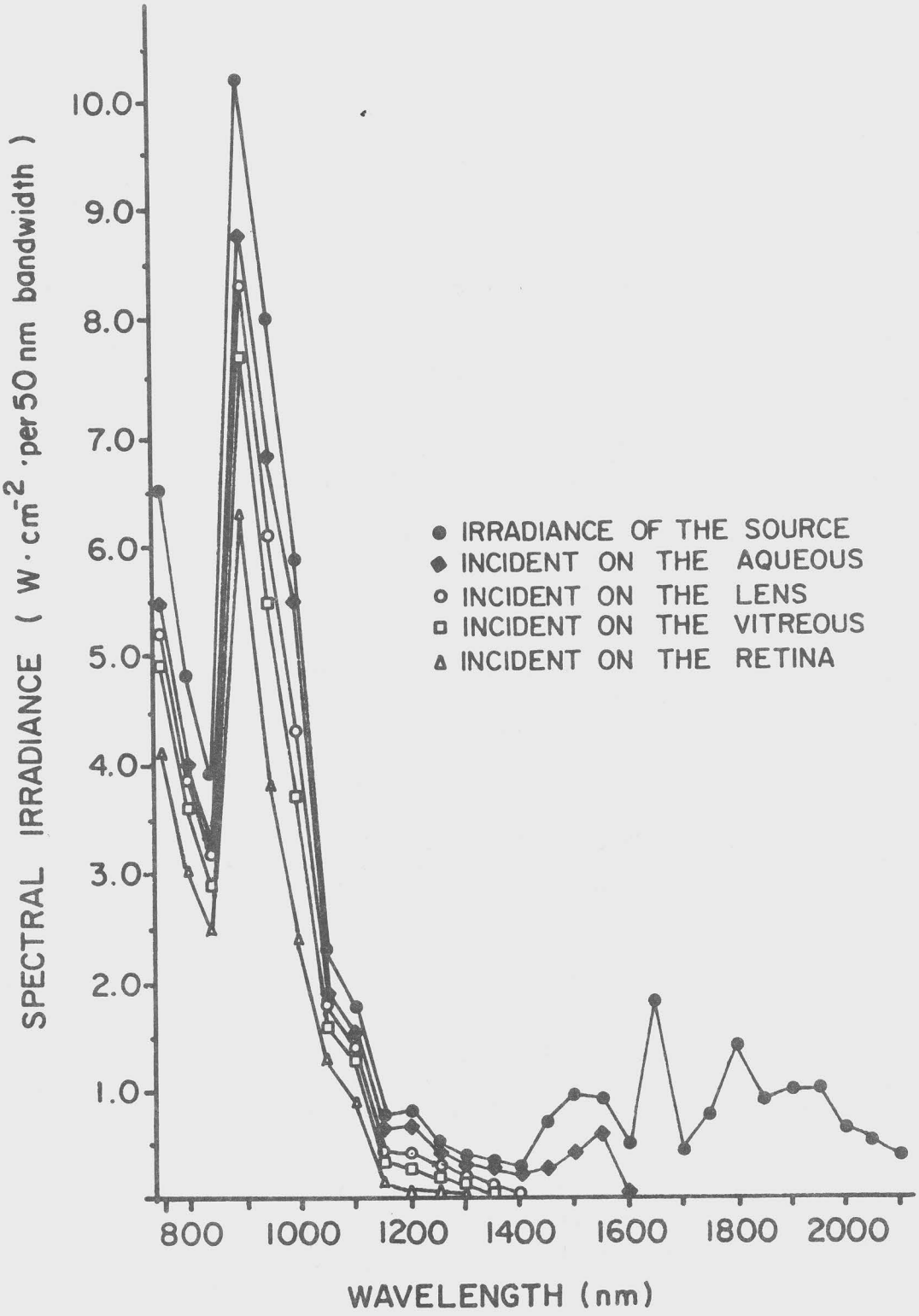

Figure 7. The spectral irradiance of the 5 kW Xenon source measured with an Eppley thermopile in 50 nm wavebands at the plane of exposure after transmittance through the Schott RG-715 filter. The irradiance incident on the aqueous, lens, vitreous, and retina was calculated from the rabbit transmittance data of Barker.[48]

To accomplish the goals of the experimental protocol, the following exposure conditions were used:

1. Infrared spectrum, unfocused beam, and normal pupil - The exposure beam was essentially collimated, and it covered the entire cornea, the iris, and the pupil since the beam was 2.5 cm x 1.5 cm in size at the plane of the cornea.

2. Infrared spectrum, focused beam, and miotic pupil - The focused exposure beam was 0.8 cm x 1.5 cm at the plane of the cornea. The miotic pupil allowed the beam to simultaneously expose the iris and the anterior lens surface through the pupil. The data were intended to study cornea, lens, and iris effects.

3. Infrared spectrum, focused beam, and normal pupil - The exposure conditions were intended to study only corneal threshold effects.

4. Infrared spectrum, focused beam, dilated (normal) pupil - The focused beam could be directed through the dilated or normal pupil to the retina. These exposures were intended to study the effects of IR exposure to the retina.

5. Full spectrum, focused beam, and miotic pupil - The focused beam allowed maximum exposure to the cornea, iris, and anterior surface of the lens. The exposures were intended to establish the full spectrum (UV, visible, and IR) effects on the cornea and the lens to study the additive or synergistic effects of the UV and visible spectrum to the IR spectrum.

6. Full spectrum, focused beam, and dilated pupil - These exposures were intended to study corneal, lenticular, and retinal damage for additive or synergistic effects of the ultraviolet or visible spectra to the IR spectrum.

The following procedures were used for each experiment:

1. Ketamine HCl, 20 mg/Kg body weight, was administered intramuscularly (IM) to the rabbit for anesthesia. For the monkey, 15 mg/Kg body weight of Ketamine HCl was administered IM. Repeat doses of 5 mg of Ketamine were given as indicated by the arousal of the animal or by excess movements of the eyes.

2. For pupillary constriction (miosis) two drops of 1% pilocarpine ophthalmic solution were instilled into the eye to be exposed at 5 minute intervals for a total of 4 drops. This procedure was accomplished approximately 20 minutes prior to the exposure of the eye to IR.

3. Pupillary dilation in the rabbit was achieved by administering two drops of 5% Homatropine followed in 5 minutes by two drops of 1% Tropicamide. Primates were given one drop of 1% Tropicamide in each eye.

4. Prior to exposure, each eye was examined thoroughly with the biomicroscope and the indirect ophthalmoscope in accordance with the Evaluation Procedures. Animals with anomalies of the anterior ocular structures (cornea, anterior chamber, iris, and lens) or the retina were rejected.

5. Rabbits were placed in a specially designed holder for exposure sessions and biomicroscopic examination. Primates were placed in a stereotaxic instrument for exposure and examination (Figure 8).

Primates were permitted to blink without restrainingthe eyelids; however, occasionally a reflex or protective ptosis of the upper lid had to be prevented by manually elevating the eyelid. Extreme care was taken to minimize corneal dehydration during this procedure. An advantage in using ketamine hydrochloride was that sensory reflexes are present and one can observe sensory responses of the animal.

Evaluation Procedures

Ocular damage criteria are given in Table I. Two observers independently examined the eye immediately after exposure to determine the criteria status and the classification for each structure of the eye as given in Table I. The criteria for the severity of the exposure for each structure was indicated as negative (-), possibly positive ($\pm$), positive (+), moderately positive (++), extremely positive (+++), and severely positive (++++) on the laboratory record sheet. If more than 50% of the criteria for any structure were positive (+), that structure was classified as above threshold (+); if 50% of the criteria for any structure were positive (+), the criteria resulted in a possibly positive ($\pm$) or threshold classification (H); less than 50% positive criteria resulted in a below threshold classification (-). The exposed eyes were examined, criteria established, and classifications made immediately after exposure, 24 hours after exposure, and at regular intervals as dictated by the severity of the damage for as long as 3 months.

After the experimental exposure and follow-up of an eye were completed, a review of the record of ocular damage was made, with all investigators present and participating, to arrive at a final classification. The final classification was based on the ocular structures damaged and the severity of the damage.

Any definite corneal, lenticular, iris, vitreous, or retinal damage was classified as positive (+). Minimal damage to the cornea, iris, lens, vitreous and retina that reversed to normal within 24 hours after exposure was classified as threshold (H). If no ocular structures were damaged, the final classification was negative (-). When a rated exposure was classified as negative and the next higher radiant exposure was classified positive but their difference was less or equal to the error of source measurement, the threshold radiant exposure (H) was calculated as the mean of these two exposures.

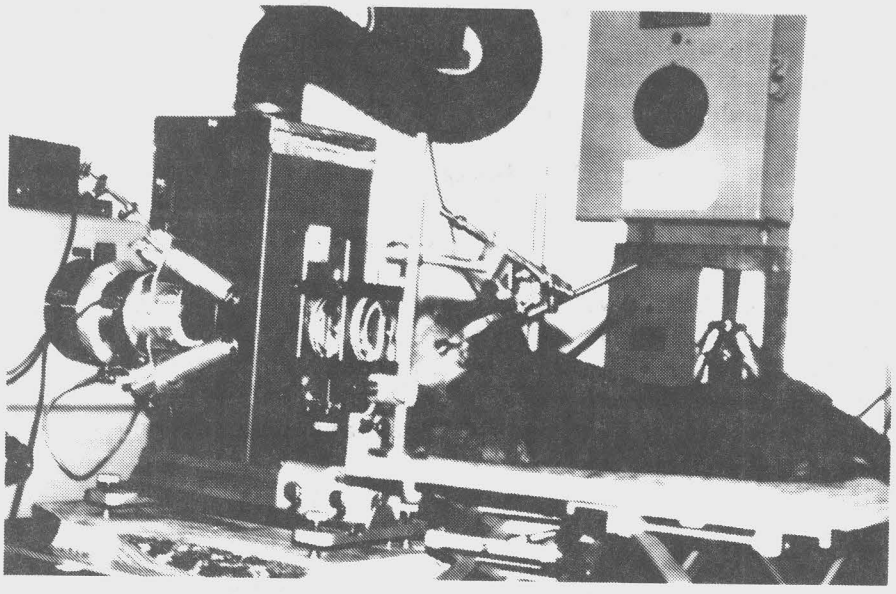

Figure 8. Cynomolgous monkey restrained in a modified stereotaxic system in the correct position for irradiation. Ketamine hydrochloride was used for anesthesia.

Figure 9. A dry swollen nictitating membrane was frequently observed following high levels of radiant exposure.

Table I. Ocular Structures Examined Pre- and Post-Exposure for Damage Criteria

	Ocular Structure	Instrument	Expected Damage
1.	Cornea	Biomicroscope	Corneal opacification, debris, haze, exfoliation
	a. Epithelium		Thickening
	b. Stroma		Haze
	c. Endothelium		Opacities
			Endothelial damage or disturbance
2.	Anterior Chamber	Biomicroscope	Aqueous flare
			Aqueous cells
			Iritic pigment in aqueous
3.	Lens	Biomicroscope	Increased prominence in anterior and/or posterior suture line
			Anterior capsular opacities
			Posterior capsular opacities
			Increased opacification of cortex and/or nucleus
			Exfoliation of the capsule
4.	Iris	Biomicroscope	Sluggish pupillary reaction
			Synechia formation, posterior
			Stromal haze
			Vascular engorgement
			Necrosis
			Exfoliation of iris stroma
			Pigmentary dispersion
5.	Vitreous Humor	Biomicroscope	Haze
		Indirect Ophthalmoscope	Opacification
			Syneresis
6.	Retina	Biomicroscope with ruby lens	Vascular disturbance
			Loss of pigment
		Indirect Ophthalmoscope	Retinal edema
			Retinal lesion (burn)

RESULTS

IR exposures were made on 100 pigmented rabbit eyes and 10 primate eyes (cynomolgous monkeys) during the experiments. The data are presented in Tables II through VI for the rabbits and in Table VII for the primates. A summary of the radiant exposures classified as threshold for the cornea, iris and crystalline lens is given in Table VIII. The exposure conditions are included in the legends for each table. The column headings for each Table provide the animal identification number, the source irradiance in $W \cdot cm^{-2}$, the exposure duration in seconds, the radiant exposure in $J \cdot cm^{-2}$, and a classification of the results of the exposure for the cornea-C, the iris-I where applicable, the crystalline lens-L, and the retina-R. The animal identification number is composed of three letters and arabic numerals; for example, IR11R or L and IP4L. The capital letter I identified the waveband of exposure as including IR, the capital R identified the animal as the pigmented rabbit and the capital P as the primate, the arabic numeral contained the number of the animal, and the R and L indicated which eye was exposed. Finally, H was used to indicate that the threshold radiant exposure had been achieved with the subscript indicating the part of the eye. The exposure durations in the results may differ slightly from that given due to rounding procedures.

It can be seen from Table II that neither corneal, iris, lenticular nor retinal threshold exposures were achieved for the IR (715 nm - 1400 nm) with an unfocused beam in spite of exposure levels exceeding the damage exposure data which are published in the literature and referenced in this report. In addition, three exposures were made using a 50 nm waveband unfocused source centered at 1050 nm. Radiant exposures to about 14,000 $J \cdot cm^{-2}$ were made without apparent effects to the cornea, iris, or lens. These results caused changes in the research protocol to include the focused beam in order to increase the irradiance at the cornea, dilated pupil to allow exposure of the lens only, miotic pupil to allow the iris and the lens to be exposed simultaneously or independently, and the use of the full source spectrum in order to compare IR exposures with exposures which contained UV and visible radiation.

The data in Table III were obtained using the 0.8 x 1.5 cm focused beam and a miotic pupil. The iris and the lens were exposed simultaneously. It can be seen that the threshold exposure for the cornea, iris and lens varies with the rate of delivery of the energy. For example, the corneal threshold exposure is close to 5000 $J \cdot cm^{-2}$ at irradiances below 40 $W \cdot cm^{-2}$ and is about 1000 $J \cdot cm^{-2}$ for irradiance levels above 4 $W \cdot cm^{-2}$. The lenticular threshold exposure decreases as the rate of delivery of the energy increases (Figure 10). At low levels of irradiance the threshold for the lens is less than that of the cornea. This means that the lens could be damaged in low levels of irradiance or very high short duration exposures, without the cornea becoming involved; however, at high levels of exposure the cornea would become damaged

Table II. Rabbit Infrared Spectrum Exposure Data Wavelength Range, Unfocused Beam, and Normal Pupils

Animal Number	Irradiance $W \cdot cm^{-2} \times 10^{-3}$	Exposure Duration-s	Radiant Exposure $J \cdot cm^{-2}$	Classification C	L	R
IR4R	32.3	167	5	-	-	-
IR3R	32.3	335	11	-	-	-
IR5L	32.3	837	27	-	-	-
IR8L	31.4	1,590	50	-	-	-
IR6R	31.4	3,180	100	-	-	-
IR10R	34.5	5,797	200	-	-	-
IR9L	43.4	6,912	300	-	-	-
IR2R	41.2	14,570	600	-	-	-
IR2L	47.9	20,895	1,000	-	-	-
IR9R	45.6	29,000	1,323	-	-	-
IR11R	48.2	29,000/day For 3 days	4,196	-	-	-
IR12R	48.3	29,000/day For 5 days	7,004	-	-	-
IR13L	66.8	29,000/day For 5 days	9,686	-	-	-

Table III. Rabbit Infrared Exposure Data Wavelength Range, Focused Beam, and Miotic Pupil

Animal Number	Irradiance $W \cdot cm^{-2}$	Exposure Duration-s	Radiant Exposure $J \cdot cm^{-2}$	Classification C	I	L	R
IR37R	2.93	1365	4000	-	H_I	H_L	-
			5500**	$+H_C$			
IR24L	2.75	2636	7250	+	+	-	-
IR25L	2.75	2636	7250	+	+	$\pm$	-
IR28R	2.75	2727	7500	$\pm$	$\pm$	-	-
IR28L	2.75	2818	7750	+	+	-	-
IR27R	2.33	3437	8010	-	+	-	-
IR27L	2.33	3652	8510	-	+to++	-	-
IR36R	3.39	960	3250	-	+	-	-
IR36L	3.39	1034	3500	-	+	-	-
IR35R	3.39	1108	3760	-	H_I	$\pm$	-
IR35L	3.39	1181	4000	-	+	H_L	-
IR34R	3.39	1255	4250	-	+	+	-
IR34L	3.39	1329	4500	-	+	+	-
IR33L	3.49	1362	4750	H_C	+	+	-
IR18L*	3.39	1475	5000	+	-	-	-
IR33R	3.49	1434	5000	+	+	+	-
IR32L	3.59	1460	5240	+	+	+	-
IR32R	3.59	1600	5740	+	+	+	-
IR16L	3.49	1912	6670	+	+	+	-
IR23L*	3.59	1877	6740	+	+	-	-
IR22L	3.59	1946	6990	+	+	+	-
IR19L*	3.49	2000	6980	+	+	-	-
IR21L	3.39	2212	7500	++	+	+	-
IR50L	4.14	637	2640	-	-	-	-
IR49L	4.14	690	2860	-	-	-	-
IR49R	4.14	734	3040	-	-	-	-
IR48L	4.14	796	3300	-	-	-	-
IR52R	4.02	870	3500	-	H_I	$\pm$	-
IR53R	4.02	870	3500	-	+	H_L	-
IR48R	4.14	849	3510	-	+	H_L	-
IR51L	3.80	986	3750	-	+	+to+	-
IR53L	4.02	933	3750	-	+	H_L	-
IR51R*	3.80	1053	4000	-	+	$\pm$	-
IR52L	4.02	995	4000	-	+	-	-
			5000**	H_C			

* Animal moved excessively during exposure.
**Mean extrapolated exposure.

Table III. continued

Animal Number	Irradiance $W \cdot cm^{-2}$	Exposure Duration-s	Radiant Exposure $J \cdot cm^{-2}$	Classification C	I	L	R
IR30R	3.81	1640	6250	+	+	+	-
IR30L*	3.81	1772	6750	+	+	$\pm$to+	
IR29R*	3.81	1903	7250	+	++	$\pm$to+	-
IR29L	3.81	2034	7750	+	++	$\pm$	-
IR59R	4.55	275	1250	H_C	H_I	-	-
IR59L	4.55	330	1500	+	+	-	-
IR58R	4.55	384	1750	+	$\pm$	-	-
IR58L	4.55	439	2000	+	$\pm$	-	-
IR57L	4.44	507	2250	+	+	H_L	-
IR57R	4.44	563	2500	+	+	$\pm$	-
IR55L	4.66	590	2750	+	+	$\pm$	-
IR56L	4.44	676	3000	+	+	+	-
IR55R*	4.66	644	3000	+	+	-	-
IR56R	4.44	732	3250	+	+	$\pm$	-
IR54L	4.66	695	3240	+	+	$\pm$	-
IR54R	4.66	751	3500	+	+	$\pm$	-

* Animal moved excessively during exposure.

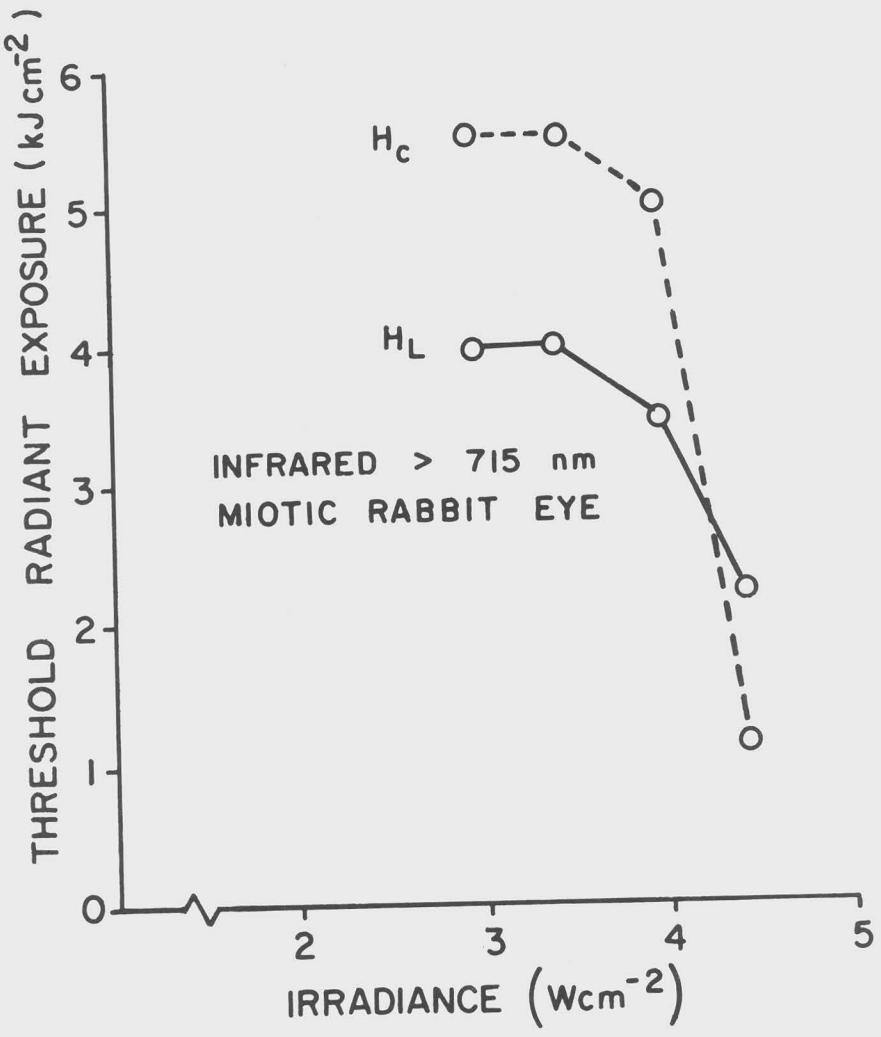

Figure 10. The threshold radiant exposure versus irradiance for the rabbit. These data show that the threshold varies with the rate of delivery of the source when the irradiance exceeds 3.5 W·cm^{-2}.

earlier than the lens. These data also demonstrate greater variability due to movements of the animal during exposure. None of the exposures caused damage to the retina.

Table IV presents the data for the IR spectrum, focused beam, and with a normal pupil. These data were intended as a check on the corneal threshold for an almost constant level of irradiance. The corneal threshold exposure was 5500 $J \cdot cm^{-2}$ for an irradiance of 3.6 $W \cdot cm^{-2}$. These data compare quite favorably with exposure values obtained using a focused beam and miotic pupil (Tables III and IV) when the $\pm$ 15% measurement error for the source is considered. An exposure at 6000 $J \cdot cm^{-2}$ with an irradiance of 2.9 $W \cdot cm^{-2}$ resulted in a slight stippling and loss of the orange peel appearance at the anterior capsule of the lens.

The effects of retinal exposure are presented in Table V. It is not possible using these data to make valid conclusions regarding the level of IR necessary to produce retinal damage. The optics of the source were not constructed for retinal effects study and extensive modification would have been necessary. When an animal was aligned to the optical beam, the beam was directed toward the band of medullated nerve fibers on the retina. Re-orientation of the animal would result in compensatory eye movements. One must be able to move the optical beam while keeping the animal stationary, to study retinal effects. Despite these limitations, a retinal burn was found in animals IR15R and IR17L and retinal damage was caused in animals IR47R and IR39L from the IR spectrum. In addition, retinal damage was found in animals exposed to the full source spectrum with a focused beam and a dilated pupil. In each instance the exposure was greater than 6000 $J \cdot cm^{-2}$ at the cornea but these data do not reflect true retinal damage exposure value for IR.

A corneal lesion as observed by the biomicroscope, progressed with increased exposure levels from an initial epithelial haze, to a stromal haze, and then to erosion of the epithelium. A qualitative description of the effects of the exposure of the rabbit eye follows:

Adnexa:

No damage to the eyelids in the rabbit was produced. A drying and swelling of the nictitating membrane (Figure 9) was a common observation at the higher radiant exposures for both IR and full spectrum radiation.

Cornea:

The corneal changes were apparent immediately after exposure. This confirmed the thermal nature of the lesion in contrast to the longer latencies found in the abiotic UV lesions. The damage to the cornea varied from epithelial haze to corneal erosion (Figure 11). All corneal damage healed rapidly, usually within 24 hours, with no scarring and the return of the cornea to a clinically normal transparency. No endothelial damage was found for the levels of radiant exposure used in these experiments.

Table IV. Rabbit Infrared Exposure Data, Focused Beam, Normal Pupil for Corneal Threshold Study

Animal Number	Irradiance $W \cdot cm^{-2}$	Exposure Duration-s	Radiant Exposure $J \cdot cm^{-2}$	Classification C	L	R
IR41R	3.39	886	3000	-	-	-
IR41L	3.39	1033	3500	-	-	-
IR37L	2.90	1380	4000	-	-	-
IR40R	3.39	1181	4000	-	-	-
IR40L	3.39	1477	5000	$\pm$to-	-	-
IR42R	3.60	1390	5000	$\pm$to-	-	-
IR43R	3.60	1460	5260	$\pm$to-	-	-
IR44R	3.60	1529	5500	H_C	-	-
IR42L	3.60	1599	5760	+	-	-
IR39L	3.39	1772	6010	+to++	-	-
IR38R	2.90	2068	6000	+	-	-
IR38L	2.90	2068	6000	$\pm$to+	-	-
IR39R	3.39	2067	7010	$\pm$	-	-

Table V. Rabbit Infrared Exposure Data, Focused Beam, Dilated Pupil for Retina Effects Study

Animal Number	Irradiance $W \cdot cm^{-2}$	Exposure Duration-s	Radiant Exposure $J \cdot cm^{-2}$	Classification C	L	R
IR17L	3.49	1891	6600	++	-	+
IR45R	3.39	2067	7010	$\pm$	-	-
IR45L	3.39	2362	8010	+	-	-
IR46L	3.81	2100	8000	+	-	-
IR47R	3.81	2100	8000	+	-	$\pm$
IR46R	3.81	2625	10,000	++	-	-
IR47L	3.81	2625	10,000	++	-	-

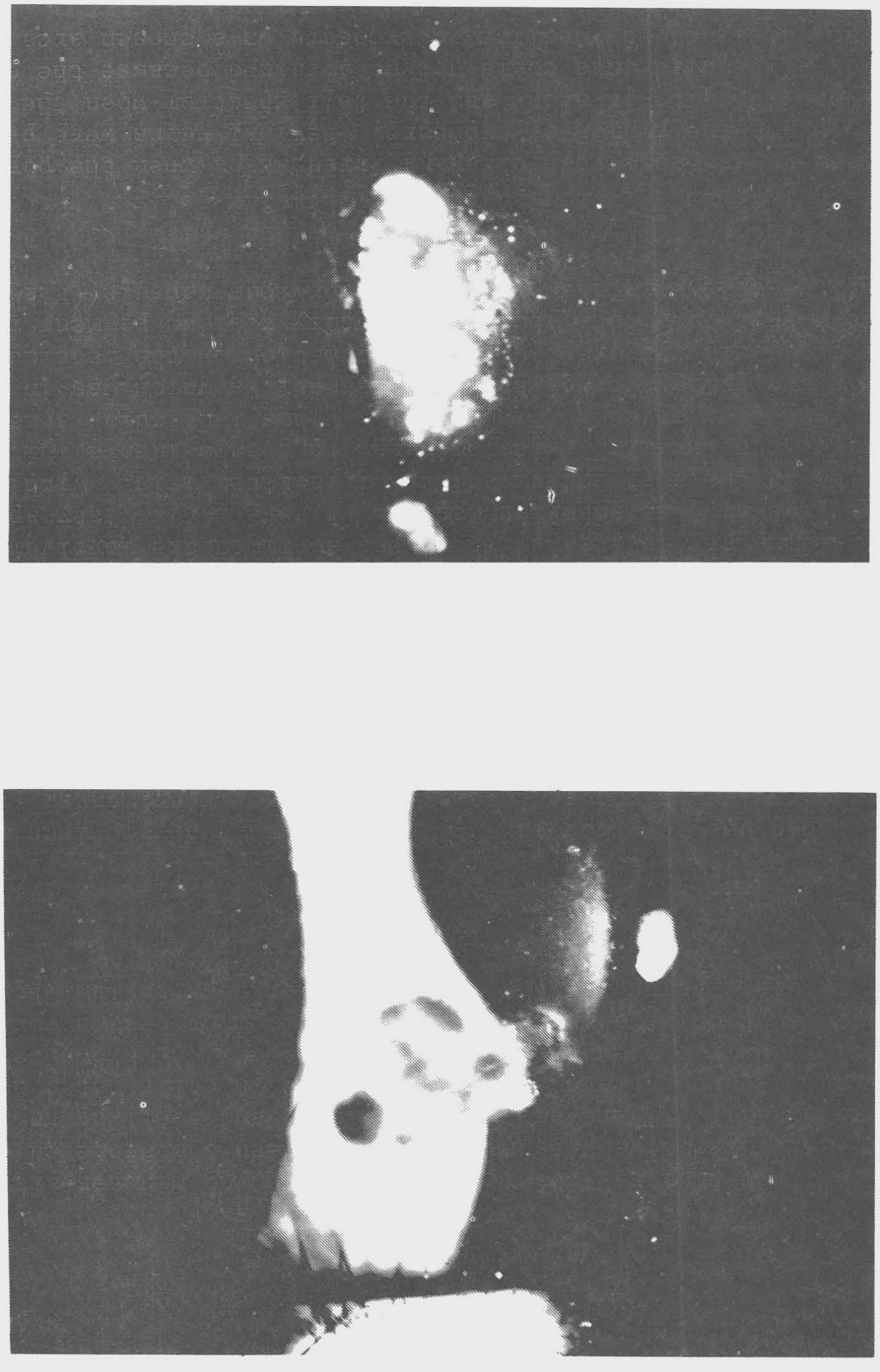

Figure 11. Infrared corneal burns showing epithelial haze, stromal haze and epithelial exfoliation.
Top: Immediately after exposure.
Bottom: One hour after exposure.

Iris:

Miosis due to irritation was observed approximately 5 minutes after an exposure began for those rabbits which had not been administered topical miotics or mydriatics. There was a stromal haze and swelling in the region of irradiation. Aqueous flare was only slight with cells noted occasionally in the anterior chamber when they could be detected. At exposure levels which produced lenticular damage, the iris involvement became more severe with the final stage being the production of fibrinous inflammatory by-products.

Lens:

Lens damage could not be produced by direct exposure of the lens to the irradiance and radiant exposure levels used in the experiments. Lens damage was easily produced when the iris overlying the lens was irradiated (Figures 12 and 13). At suprathreshold levels of radiant exposure, the anterior capsule and anterior stroma became slightly hazy and a few minute subcapsular opacities were found. The characteristic progression of the lesions for higher levels of radiant exposure is shown in Figure 13. The involvement of the overlying iris was considerable with exfoliation of the posterior pigment onto the anterior capsule of the lens together with fibrinous inflammatory material. There was an immediate involvement of the anterior lens and the anterior capsule (Figure 14A). They appeared hazy and white in the area underneath the irradiated iris. Within 1½ hours after exposure, the lenticular lesion began to change into a white opacity surrounded by an area of haze (Figure 14B). This lenticular area corresponded to the overlying area of the irradiated iris which was in contact with the lens capsule (Figure 14C). The formation of the lenticular opacity was complete within one month, but occasionally residue pigment from the posterior of the iris remained on the anterior lens capsule (Figures 15 and 16).

Retina:

No retinal damage was observed following irradiation when the pupil had been miotic during the period of exposure. Retinal burns were produced (Figures 17 and 18) with IR alone and the full spectrum when the pupils were dilated. Threshold data could not be obtained because the exposure system was not designed to localize an exposure on a chosen area of the retina.

Table VI provides data for rabbit full spectrum, focused beam with miotic and dilated pupils. The purpose of these experiments was to determine if UV and visible radiation were additive or synergistic with IR. The threshold radiant exposure was about 750 $J \cdot cm^{-2}$ for the cornea and 2250 $J \cdot cm^{-2}$ for the lens. These threshold values may be compared with a corneal radiant exposure of less than 1200 $J \cdot cm^{-2}$ and a lenticular radiant exposure of 2250 $J \cdot cm^{-2}$ using only IR and equivalent exposure conditions in Table VIII.

Low levels of IR exposure produced no obvious subjective signs in the rabbit. As the exposure levels increased, a reflex blepharospasm of the lids and

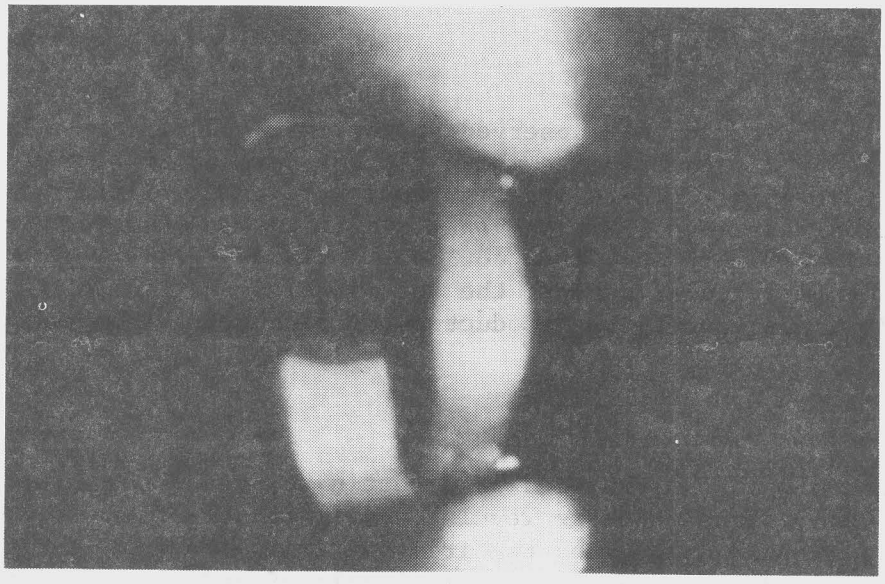

Figure 12. Extreme swelling of the iris stroma with ectropion of the uveae. The radiant exposure was 12,500 $J \cdot cm^{-2}$ delivered in 2567 s (IP5R) with an irradiance at 4.87 $W \cdot cm^{-2}$.

Figure 13. Narrow strip of iris pigment is seen adherent to the anterior capsule of the lens. Radiant exposure was 12,500 $J \cdot cm^{-2}$ delivered in 2567 s with an irradiance of 4.87 $W \cdot cm^{-2}$ (IP5R). One month after exposure.

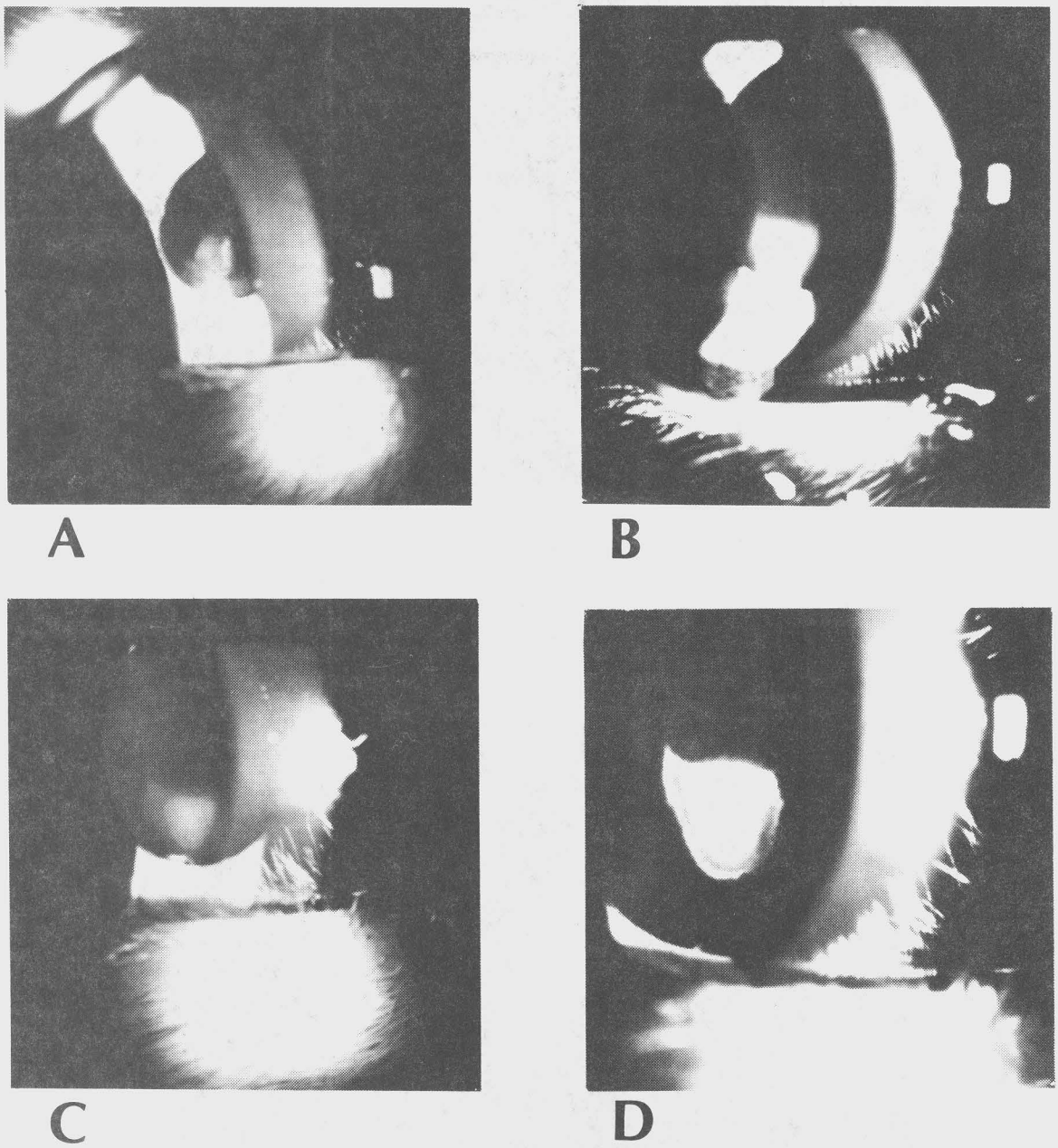

Figure 14. Characterisitc progression of lenticular opacities in the rabbit.

A. Epithelial haze, stromal haze of the iris, opacification of the lens in the irradiated area underlying the iris.
B. Discrete lenticular lesion surrounded by haze, upper border corresponds to the lower border of the pupil. Pigment spots and fibrinous inflammatory material seen just above pupillary margin.
C. Lenticular lesion has become well organized.
D. Lesion characteristic of IR or full spectrum exposure. Iris involvement is greatly reduced with only a small marginal tuft apparent. IR31R, 2250 $J \cdot cm^{-2}$, 484 s, full spectrum, miotic pupil at an irradiance of 4.66 $W \cdot cm^{-2}$.

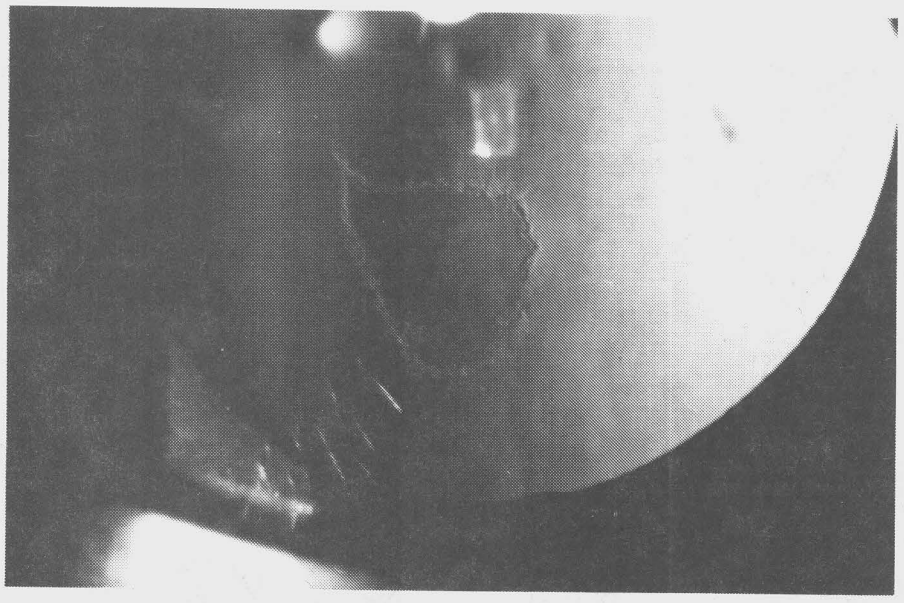

Figure 15. Retroillumination of the lenticular opacity shown in Figure 14D reveals the granular nature of the perimeter of the lesion. The translucency of the center of the lesion suggests that the disturbance is intrafibrillular rather than structural damage or protein coagulation of the lens fibers (IR31R).

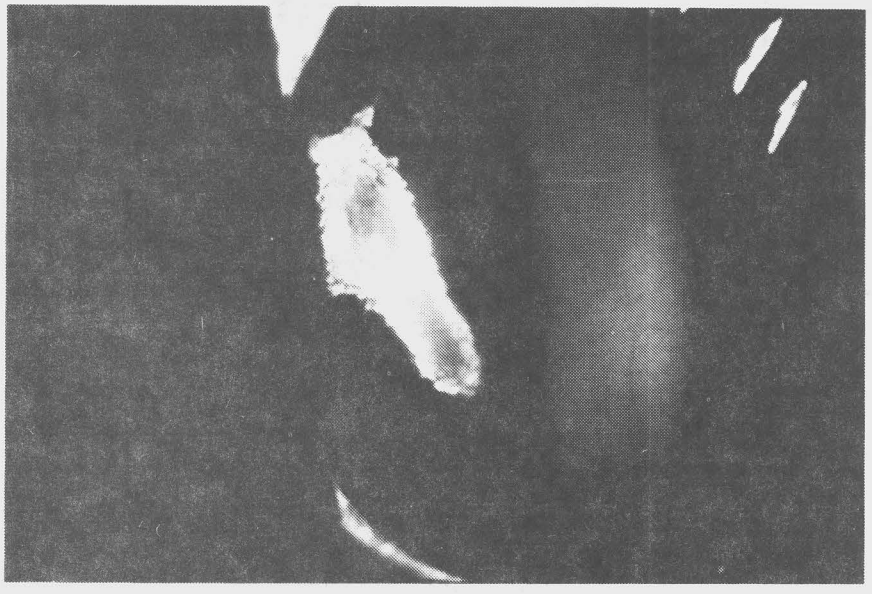

Figure 16. Lenticular lesions of the rabbit from exposure of the overlying iris with 8030 $J \cdot cm^{-2}$ in 1800 s to the full spectrum beam with a miotic pupil. Lesions such as these were consistently reversible within 4 weeks (IR15R). The irradiance was 4.46 $W \cdot cm^{-2}$.

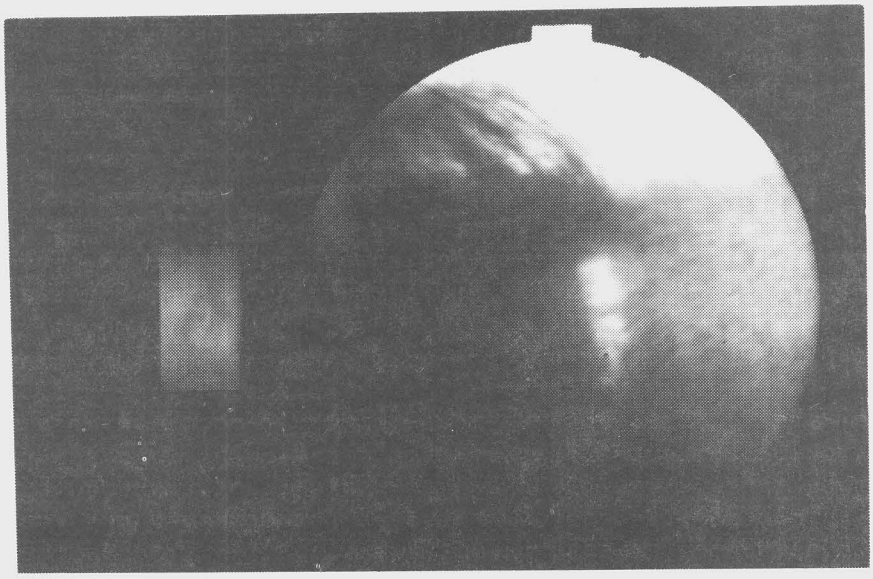

Figure 17. Rabbit chorioretinal lesion produced through a dilated pupil. The central burn is surrounded by severe retinal edema. Radiant exposure was 6600 $J \cdot cm^{-2}$ of infrared radiation measured at the cornea and delivered in 1891 s (IR17L) with an irradiance of 3.49 $W \cdot cm^{-2}$.

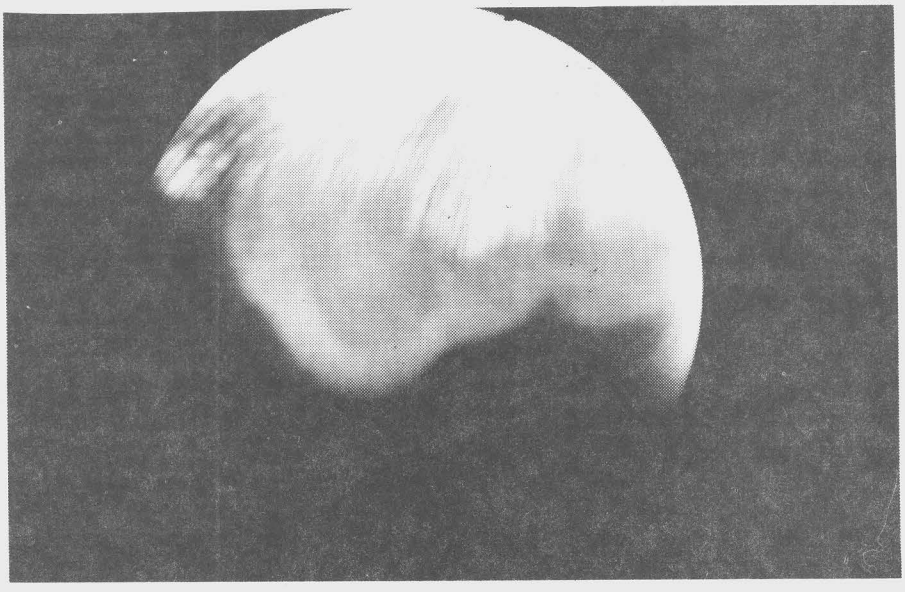

Figure 18. Severe chorioretinal burn of the rabbit retina produced through a dilated pupil. The radiant exposure was 6000 $J \cdot cm^{-2}$ full spectrum measured at the cornea and delivered in 1288 s (IR17R) with an irradiance of 4.66 $W \cdot cm^{-2}$.

Table VI. Rabbit Full Spectrum Exposure Data

Animal Number	Irradiance $W \cdot cm^{-2}$	Exposure Duration-s	Radiant Exposure $J \cdot cm^{-2}$	Classification C	I	L	R
A. Focused Beam, Miotic Pupil							
IR26R	3.81	52	200	-	-	-	-
IR26L	3.81	131	500	-	-	-	-
			750*	H_C			
IR25R	3.81	262	1000	+	H_L	-	-
IR31L	4.65	258	1200	+	+	+	-
IR24R	3.81	525	2000	+	+	$\pm$	-
IR19R	4.66	429	2000	+	+	H_L	-
IR23R	4.66	483	2250	+	+	+	-
IR31R	4.66	484	2250	+	+	+	-
IR22R	4.66	536	2500	+	+	+	-
IR21R	4.46	673	3000	+	+	+	-
IR18R	4.66	858	4000	++	+	+	-
IR15R	4.46	1800	8030	++	++	+	-
B. Focused Beam, Dilated Pupil							
IR17R	4.66	1288	6000	+	-	-	+
IR20R	4.66	1800	8390	+	-	-	+
C. Unfocused Beam, Miotic Pupil							
IR15L	0.11	7200	790	+	-	-	-
IR14L	0.16	7200	1150	+	+	-	-

* Mean extrapolated exposure

miosis of the pupil in normal animals were found. The total spectrum exposures were accomplished only at relatively high levels of irradiance and produced extreme photophobia, reflex blepharospasm, and pupillary constriction. There was a tendency for the rabbit cornea to become "dry" and corneal damage from exposure was evident at lower radiant exposure levels when the "drying" occurred. The results of "drying" were a loss of corneal transparency, lowered corneal radiant exposure thresholds, and an effective protection of the iris and lens resulting in the raising of their radiant exposure thresholds.

The rabbit data generally showed greater variability because it took time to devise an adequate restraint for the eyelids. In early exposures some rabbits had no restraint of the lids and responded with a protective ptosis, a partial closure of the nictitating membrane, or a complete closure of their eyes. Restraint of eyelid movements was attempted by using an ocular speculum, by using surgical tape to hold the lids open, and by using fixation sutures in the anterior part of the ocular globe. The ocular speculum was abandoned quickly because the interruption of the tear flow across the cornea resulted in corneal drying affecting the exposure levels. Taping the lids open was the method adopted because it allowed better control of the tear flow and reduced the subsequent drying of the cornea.

The primate exposure data are given in Table VII. The radiant exposure levels required to achieve a threshold response were 8000 $J \cdot cm^{-2}$ for the cornea and iris and 12,500 $J \cdot cm^{-2}$ for the lens. These values are considerably higher than those found for the rabbit. All primate exposures included the iris and part of the pupil with the focused beam. A qualitative description of each of the ocular components should assist in understanding the result:

Adnexa:

No damage occurred in the eyelids of the monkey.

Iris:

The iris involvement was essentially the same as that for the rabbit.

Cornea:

At irradiance levels above 4.0 $W \cdot cm^{-2}$, the blink rate of the monkey increased and probably afforded some protection to the cornea. It was felt that the increased blink rate was caused by reflex activity induced by increased heating of the cornea. Other effects observed were increased epithelium debris and haze. No significant corneal disturbance was produced until the radiant exposure attained 8000 $J \cdot cm^{-2}$; however, these signs may have resulted from forcibly opening the eye (with normal lid position) because of the excessive blinking. Nevertheless, higher levels of radiant exposure resulted in more severe damage which included granules, stippling, epithelial haze, and stromal haze.

Table VII. Primate Infrared Exposure Data, Focused Beam, and Miotic Pupil

Animal Number	Irradiance $W \cdot cm^{-2}$	Exposure Duration-s	Radiant Exposure $J \cdot cm^{-2}$	Classification C	I	L	R
IP1L	4.55	440	2000	-	$\overline{+}$	-	-
IP2L	4.55	494	2250	-	$\overline{+}$	-	-
IP2R	4.55	549	2500	-	$\overline{+}$	-	-
IP1R	4.55	604	2750	-	$\overline{+}$	-	-
IP3R	4.87	718	3500	-	$\overline{+}$	-	-
IP3L	4.87	1437	7000	-	$\overline{+}$	$\overline{+}$	-
IP4R	4.23	1891	8000	H_C	H_I	$\overline{+}$to+	-
IP4L	4.23	2364	10,000	$\overline{+}$to+	+	H_L	-
IP5R	4.87	2567	12,500	$\overline{+}$	+	+	-
IP5L	4.87	3080	15,000	+	+	+	-

Iris:

No damage to the iris was found until a radiant exposure of 8000 $J \cdot cm^{-2}$ was reached. At this radiant exposure a localized stromal haze of the iris was seen. The stromal haze increased and swelling was seen at the 10,000 $J \cdot cm^{-2}$ radiant exposure. At 12,500 $J \cdot cm^{-2}$, flare was seen in the anterior chamber and there was an extreme swelling of the iris stroma with ectropion of the uvea (Figure 16). One month later, a narrow strip of pigment was seen adherent to the anterior lens capsule (Figure 17). This pigment probably represented remnants of the posterior pigment epithelium of the iris and indicated an old inflammation of the iris.

Lens:

No lenticular damage was produced by direct irradiation of the lens through the pupil at exposure levels up to 15,000 $J \cdot cm^{-2}$. With radiant exposures of 8000 $J \cdot cm^{-2}$ and 10,000 $J \cdot cm^{-2}$ through the iris, only very subtle lens changes were detected. These included a few minute subcapsular opacities at 10,000 $J \cdot cm^{-2}$ which were visible only with high magnification and specular reflection. Subcapsular haze and discrete opacities of the primate lens were found with radiant exposures of 12,500 $J \cdot cm^{-2}$ (Figure 16). No permanent cataracts were produced.

Retina:

No retinal damage occurred to the primates during exposure.

Table VIII summarizes the threshold exposure data for the cornea, iris, and the lens using the IR spectrum and the full spectra, and with miotic or dilated pupils for both the rabbit and the primate. These data demonstrate that the radiant exposure depends on the level of irradiance for the IR spectrum. The radiant exposure to attain a threshold response for the primate requires an increase of a factor of about 8.0 when compared to the rabbit. These data also show that with equal levels of irradiance, the rabbit radiant exposure threshold compares favorably for both the IR and full spectra exposures.

Table VIII. Summary of All Threshold Radiant Exposure ($J \cdot cm^{-2}$) Data for the Cornea, Iris, and Lens

Irradiance ($W \cdot cm^{-2}$)	Cornea	Iris	Lens
A. Rabbit Infrared Spectrum, Focused Beam, Miotic Pupil (Table III)			
2.3 - 2.9	5500	4000	4000
3.4 - 3.6	4750	3760	4000
3.8 - 4.1	5000	3500	3500
4.4 - 4.7	1250	1250	2250
B. Rabbit Full Spectrum, Focused Beam, Miotic Pupil (Table VI)			
3.8	750	1000	2000
C. Primate Infrared Spectrum, Focused Beam, Miotic Pupil (Table VII)			
4.2 - 4.9	8000	8000	10,000

DISCUSSION

The mechanism of the formation of IR cataracts has centered around three hypotheses. Vogt (15, 16) interpreted his data to indicate that the IR induced cataracts were the result of the direct absorption of the radiant energy by the crystalline lens. There is some experimental evidence to support Vogt since ocular transmittance measurements demonstrate absorption bands of IR in the 800 nm to 1200 nm bandwidth. However, Vogt's own description of the source used to expose the animals could negate these interpretations. Vogt described the source as a carbon arc (Bogen lamp) "whose light was filtered through water, iodine and carbon disulfate" (deren Lict durch Wasser und Jod schwefelkohlenstoff filtriert wurde) (16). It is known that water absorbs IR in bands much like the aqueous and the vitreous, thus reducing the IR available for absorption by the anterior segment of the eye. Furthermore, iodine readily transmits the UV radiation produced by the carbon arc lamp. Vogt's descriptions of conjunctivitis and lenticular opacities are the same as those found for UV exposure (37). Thus, it is suspected that the direct absorption by Vogt's animals was UV radiation rather than IR.

Verhoeff and Bell (9) suggested that the Vogt hypothesis was not sufficient. They argued that the outer surface of the cornea was air cooled and that the anterior capsule of the lens was cooled by circulation of the aqueous; thus, the cataract formed on the posterior surface of the lens. They further postulated that the heat interfered with the function of the ciliary body which subsequently interfered with the metabolism of the crystalline lens. Nearly every researcher, including Verhoeff and Bell, has reported anterior lenticular opacities and corneal involvement. Therefore, the air and aqueous are not sufficient to prevent anterior lens and corneal involvement. If the ciliary body was damaged some evidence should be seen in the aqueous and very little or no aqueous involvement has been observed. Thus, it appears that the model of Verhoeff and Bell, also, does not account for the experimental evidence. On the other hand, in many experiments the cornea could be dry during the exposure.

The actual mechanism of the formation of IR cataracts was probably proposed by Goldmann (17-24). He interpreted his research to indicate that the subsequent cataract was due to the IR being absorbed by the iris and the indirect transmittance of the heat to the lens. Goldmann believed that the effects of the direct absorption of the IR were minimal. The experimental evidence accumulated has been substantially in favor of the hypothesis of Goldmann (30). Some research (38, 39) suggests that both direct absorption by the lens and indirect heating of the lens through the absorption of the iris account for IR induced cataracts. Our research supports the hypothesis of Goldmann because we were not able to produce a lenticular opacity by directly exposing the lens but obtained lenticular opacities only when the iris was exposed and then the opacity was directly beneath the area of the exposed iris. The contribution of direct exposure to the lens appears to be minimal.

What does an IR induced cataract or lenticular opacity look like? Where is the lenticular opacity located within the crystalline lens? Meyenhofer (11) described the chronic exposure "glassworker's cataract" as a posterior cortical opacity which took the shape of "stars." Edbrooke and Edwards (40) contended that heat-induced cataracts started with an initial cobweb-like appearance and developed into a well-defined opacity in the outer layers of the posterior cortex of the crystalline lens. Vogt (15, 16) described grayish dots in the anterior lens epithelium from acute exposure which progressed to a posterior subcapsular opacity. Verhoeff and Bell (9) reported that the initial response was a mitosis of the lens epithelium in the area beneath and in contact with the iris pigment epithelium. They also described the posterior subcapsular opacity as a later phase of development. Goldmann's description (19) was almost identical to that given by Vogt. Langley, Mortimer and McCullough (30) described the clinical appearance as beginning in the region of exposure under the iris as diffuse, fine gray anterior subcapsular dots with iris pigment which may be adherent to the anterior lens capsule. The next stages involved clouding of the equator, migration into the anterior cortex of the anterior grayish dots, the appearance of a saucer-shaped posterior opacity, and the joining of the anterior cortex-equator-posterior complex into a "U" shaped opacity. Their conclusion was that the posterior lenticular opacity had a latent period of 60 to 90 days.

The latent period for the cataract to develop may assist in establishing whether or not the lenticular opacity was caused by IR. If the lesion was induced by IR through the action of heat or temperature, the lesion should occur immediately after the exposure achieved or exceeded threshold. Vogt's description of the anterior lens epithelium dots indicated that they were the initial mitotic response and most certainly occurred within the first 24 hours. Goldmann also described the anterior subcapsular changes as an immediate or an initial response. Langley, Mortimer and McCulloch stated that their fine gray anterior subcapsular dots occurred within 24 hours. In our present study, the latency for the threshold response was as short as 1½ hours and never as long as 24 hours but almost consistently close to 6 hours after exposure. It appears that most of the research has demonstrated anterior lens epithelium dots or granules occurring almost immediately after exposure and not more than 24 hours after exposure.

It appears that the anterior subcapsular opacity is common to almost all types of radiation induced cataracts. Cogan, Donaldson and Reese (41) described the characteristics of the x-ray, the atomic bomb, and the cyclotron exposure induced cataracts. The initial or least advanced lesion consisted of spottiness and attenuation of the anterior subcapsular epithelium. There was a piling up of the equatorial cells with the failure of these cells to "drop off" into the cortex. The advanced stage in humans as seen with the ophthalmoscope was a doughnut-shaped configuration with sharply demarcated anterior boundary and a bivalve configuration. This description is very similar to the IR cataract progression given by Langley et al. (30). Duke-Elder (42) stated that the most interesting type of cataract was that caused by ionizing radiation, including x-rays, β-rays, γ-rays, and neutrons.

Histologically, the anterior subcapsular epithelium was primarily involved along with secondary involvement of the cells of the equatorial area of the lens. The UV induced lenticular opacity was described as small, circumscribed white spots located in the anterior epithelium just posterior to the anterior capsule (37). The experimentally induced IR opacity appeared similar to the UV induced opacity (9, 37) and was located in the anterior lens epithelium (9, 30, 37). The preponderance of experimental evidence describes the radiation induced cataract of both ionizing and non-ionizing radiation as an anterior epithelial opacity.

The experimental evidence in the literature indicates that the acute IR induced lenticular opacities are not the "classically described posterior subcapsular opacities" that develop with a latency of 60 to 90 days. Past research and our present study indicate that the acute IR induced opacities lie in the anterior subcapsular or anterior epithelium of the lens. The acute opacities appear as discrete "whitish dots" or granules. If a sufficient exposure has been given, the granules or whitish dots form into a diffuse whitish opacity. We have followed exposed eyes for up to 45 days and did not observe the migration of the anterior opacities either equatorily or posterior subcapsularly into the anterior cortex but, instead, the anterior opacities faded and disappeared within 6 weeks after exposure. Pitts and Cullen (37) have described a posterior subcapsular lenticular opacity in the normal rabbit. The posterior opacity followed the posterior suture horizontally as far as the equator and could be described as saucer-shaped in appearance. Often, the posterior opacity projected a white filament anteriorly from the posterior pole to the lens nucleus and, occasionally, the lens nucleus took on a diffuse, whitish appearance. The posterior subcapsular cataract, found in 100% of our laboratory rabbits, took on a denser appearance as the animal aged, much like the classical description of the IR cataract. We must emphasize that none of the lenticular opacities induced by either full spectrum or the IR spectrum exposures were posterior subcapsular opacities. For the above reasons, we conclude that the IR induced cataract is an anterior subcapsular opacity while the posterior subcapsular opacity is due mainly to the normal aging process which may or may not be accelerated by the exposure to IR.

If it were accepted that the experimental evidence of the present study proves that the anterior epithelial opacities are caused by IR, an explanation of the origin or development of the "classical posterior subcapsular cataract" is needed. The epidemiological literature left no doubt that the number of workers in the iron, steel, glass and rail industries who have developed the "IR or heat induced posterior subcapsular cataracts" exceeded the number of workers in other industries. This is particularly evident in the epidemiological literature of the late 1890s and early 1900s (12, 25). Beginning in the 1920s, epidemiological studies (27, 33) seem to indicate that workers in the "heat industries" show equal or fewer cataracts than control populations. What was the cause of this change? First, statistical procedures in handling epidemiological data had improved by the 1920s. One example is the study of Hiller et al. (43)

on the incidence of cataracts caused by sunlight. Their excellent study warns that definitive conclusions cannot be made because only inadequate records of cataract incidence and surgery were available. It is to be noted that if sunlight were the causative agent, UV radiation would necessarily be implicated because the atmosphere transmits radiation down to 295 nm and the 295 nm - 320 nm wavelength range comprises the ultraviolet action spectrum for cataracts. Finally, the decrease in incidence of IR cataracts from the worker's environment may be due to improved environmental conditions including protective devices for the eyes, automation of the manufacturing processes, and probably better dietary habits of the worker.

Most experiments that report posterior subcapsular cataracts used massive radiant exposure levels. Duke-Elder (2) reported Meesman as stating that his radiant exposures were "3 $cal \cdot cm^2 \cdot sec^{-1}$ equal to 30 or more hours of radiation over 4 months." This calculates to a radiant exposure of 1.4×10^6 $J \cdot cm^{-2}$ which is an extremely high exposure and approximately a factor of 100 above any exposure given during this study. Other researchers do not give measurements of their source but the description of the damage which resulted from their exposures indicates massive exposures. One should not forget that there are two phases to coagulation. The first phase is denaturation, a chemical change that involves hydrolysis. The second phase involves the flocculation of the denatured molecules in which coagulation occurs, perhaps by a physical process. These two processes may be separated by an indefinite period of time. Thus, the IR could be absorbed by the anterior epithelium of the lens and denaturation would occur. The white dots or grayish anterior haze would represent the denaturation process. The coagulation process is completed when the posterior lens material becomes opaque. The degree of opaqueness is related to the health of the individual and the level of radiation absorbed. The posterior subcapsular cataract would represent the agglutination portion of the coagulation process. Under this scheme, damage to the anterior lenticular epithelium by the absorption of the IR results in an increase in the posterior subcapsular cataract. Thus, the size and density of the posterior opacity might depend on the initial damage to the anterior epithelium. Since our radiant exposures were intended to determine threshold exposures, subsequent posterior cataracts were not found in our experiments. This analysis would account for the extensive delay in the development of the posterior subcapsular cataract which has been reported in the literature in spite of the fact that faint opacities occur naturally in the rabbit.

The irradiances used for the exposures during this study varied from 0.002 to 4.7 $W \cdot cm^{-2}$ and the majority of the exposures compare favorably with the 0.02 to 0.4 $W \cdot cm^{-2}$ irradiance levels experienced by glassworkers, steel workers, brass workers, arc welders, and locomotive firemen. Despite these comparisons, the present data must be considered as reflecting acute rather than chronic exposure since most animals were exposed once and observed for only about 10 days. The total radiant exposure received by an animal during a single experiment might not equal the constant exposure received by a worker over years on the job. However, it appears that if protection were provided for the worker based on acute exposures, the chronic factors might be alleviated.

It is difficult to compare data from various researchers for many reasons. Most researchers have failed to define their source and, therefore, one cannot be certain of the limits of the spectrum. Many researchers did not even measure the irradiance of their sources and provided only the durations of their exposures and the ocular damage which resulted. Many used sources which were thought to be only IR in output but have subsequently been shown to include more visible and UV radiation than the IR which was being studied. Even when the irradiance, exposure duration, radiant exposure, and wavelength range of the source are given, it becomes impossible to compare data. For example, Jacobson et al. used a 1600 W Xenon lamp to establish the corneal threshold at 5.8 $J \cdot cm^{-2}$ for the wavelength range of 800 nm to 1670 nm with an irradiance of 34.2 $W \cdot cm^{-2}$ for duration of 150 ms. The corneal radiant exposure threshold in this study was 5500 $J \cdot cm^{-2}$ using a source with an irradiance of 3.6 $W \cdot cm^{-2}$ delivered over a duration of 1529 s using a source size of 0.8 cm x 1.5 cm (1.2 cm^2) at the plane of the cornea (Table IV). Which data are correct? Both sets of data are correct because of the source differences. The source of Jacobson et al. had an irradiance which was a factor of 9.5 greater than the irradiance of our source. Jacobson's et al. exposure was delivered in 150 ms, a factor of 10,000 less than the duration of the exposure in our experiments. Finally, the size of the images at the plane of the cornea differed greatly. Hence, one may contrast but not compare the effects of the two different exposures.

The rabbit data in Figure 10 may assist in a further understanding of the differences between certain studies. It appears that as long as the IR source irradiance is 3.5 $W \cdot cm^{-2}$ or less and the source area remains constant, there is little difference in minimal lesion exposures. As the irradiance exceeds 4 $W \cdot cm^{-2}$, the radiant exposure decreases by a factor of 4.0 for the cornea and by a factor of about 2.0 for the lens with all other experimental variables held constant. Furthermore, the differences between the full spectrum data and the IR spectrum data for higher irradiances are minimal. This indicates that the visible and UV spectra combined with the IR spectrum are not synergistic but additive because almost identical threshold exposures are found for both conditions. Thus, these data would indicate that the damage was due to heat from the absorbed radiant energy and as long as the irradiance or rate of delivery exceeds a certain level, the damage should occur over a given exposure duration regardless of the spectral distribution of the source. These data indicate that the visible and UV radiation must be considered when establsihing protective criteria and formulating safety standards, especially for the IR region.

Figure 19 shows the radiant exposure in $J \cdot cm^{-2}$ versus the exposure duration in seconds required to reach threshold damage. The plot can be represented by a straight line whose formula $y = 2.83 x + 619.5$ indicates that the threshold radiant exposure H_L may be calculated by multiplying the irradiance by 2.83 and adding the constant 619.5. The straight line characteristics of these data are taken to indicate that a single process was in operation during exposure which produced the minimal observable lesion. All evidence from these experiments indicate that heat is probably the causative agent. The data also demonstrate that in spite of the different

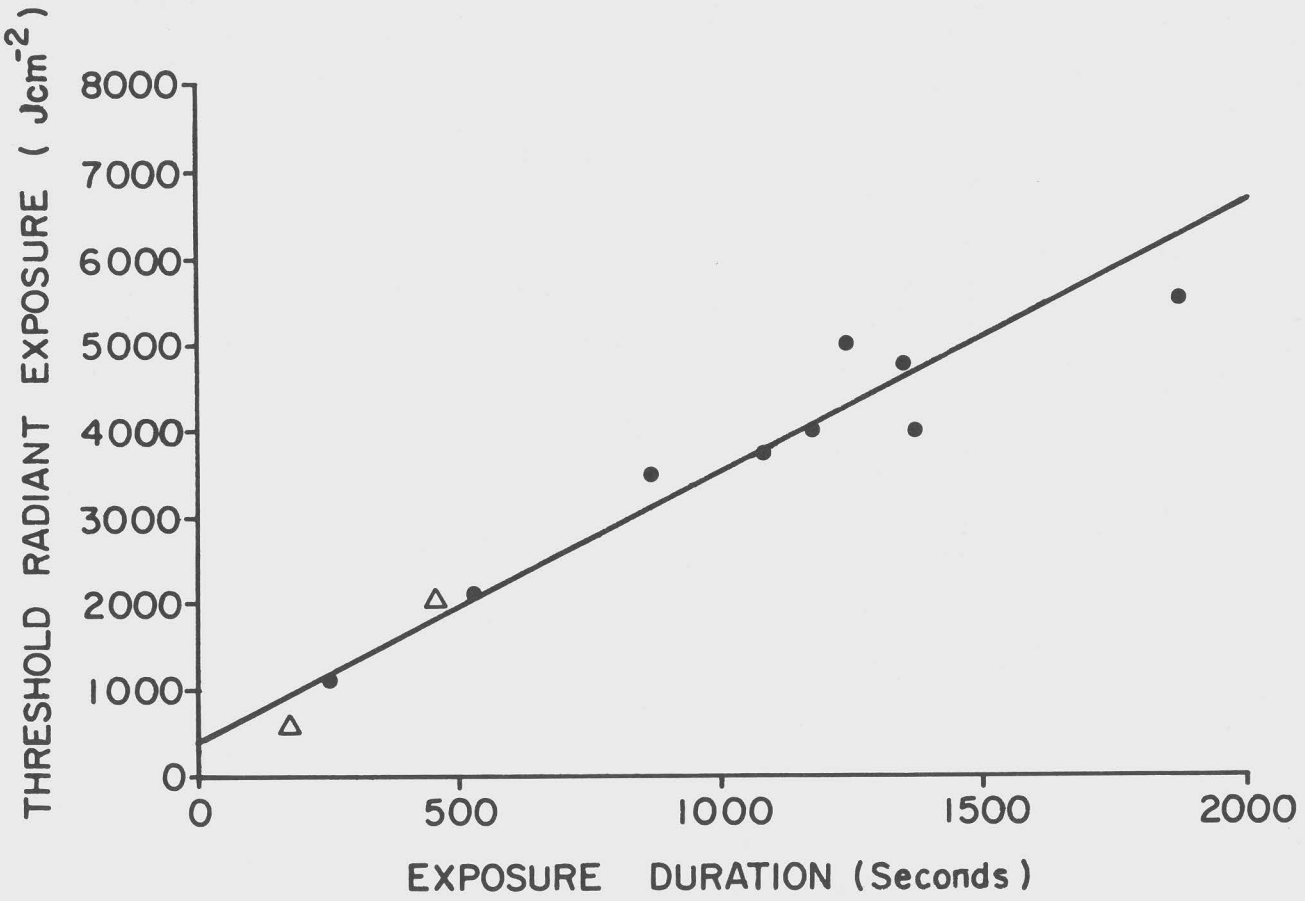

Figure 19. Radiant exposure required to produce a minimal lesion in the rabbit eye for different exposure durations. H_L in $J \cdot cm^{-2}$ is plotted on the ordinate and exposure duration in seconds along the abscissa. The symbol (o) represents data for the IR spectrum, focused beam, and miotic pupil while the (Δ) is the data for full spectrum, focused beam, and miotic pupil.

irradiance levels and exposure durations used during experimentation the evaluation criteria and procedures arrived at a fairly uniform and consistent threshold value.

Based on the above it can be stated that the threshold radiant exposure for the IR spectrum, above 700 nm with a 1.2 cm^2 source image at the plane of the cornea and a source irradiance below 3.9 $W \cdot cm^{-2}$ was 5000 $J \cdot cm^{-2}$ for the cornea, about 3500 $J \cdot cm^{-2}$ for the iris, and 4000 $J \cdot cm^{-2}$ for the lens. As the source irradiance exceeded 4.0 $W \cdot cm^{-2}$ the threshold radiant exposure was 1250 $J \cdot cm^{-2}$ for the cornea, 1250 $J \cdot cm^{-2}$ for the iris, and 2250 $J \cdot cm^{-2}$ for the lens. The radiant threshold exposure for the full spectrum from the source was 750 $J \cdot cm^{-2}$ for the cornea, 2250 $J \cdot cm^{-2}$ for the iris, and 2250 $J \cdot cm^{-2}$ for the lens.

The monkey IR exposure data are approximately a factor of 6 above the rabbit data (Tables VII and VIII). It is difficult to account for such a large increase in threshold exposure but several factors may combine to account for at least part of the increase. The stroma of the iris of the monkey is much more vascular than that of the rabbit and, consequently, as the primate iris heats up, the vessels dilate, allowing more blood to pass and adding the the cooling capacity of the iris. The stroma of the monkey iris is thicker, denser, and more pigmented than that of the rabbit and these factors, along with increased blood flow, would dissipate heat prior to its reaching the iris pigment epithelium. Although the above factors should serve to increase the monkey threshold it is difficult to conceive of such a large increase in threshold. The increased transmittance by the primate cornea may offset at least some of the effects noted. Hence, the reasons for the increase in the primate threshold remain largely unsolved.

Retinal lesions were produced with a corneal irradiance of 3.5 $W \cdot cm^{-2}$ for a duration of 1288 s with a corneal radiant exposure of 6000 $J \cdot cm^{-2}$ (Figure 17, IR17R) and for an exposure duration of 1891 s with a corneal radiant exposure of 6600 $J \cdot cm^{-2}$ (Figure 16, IR17L). The area of the source at the cornea was calculated to be 0.035 cm^2 with the retinal irradiance of 29.7 $W \cdot cm^{-2}$ if a 0.7 cm pupil and 0.70 integrated transmittance was assumed. The retinal lesion was discrete and seen 24 hours after exposure.

Ham et al. (44) exposed the rhesus monkey to the same wavelength range of IR and produced a threshold retinal lesion with a retinal irradiance of 23.4 $W \cdot cm^{-2}$ from a retinal image diameter of 1000 μm (0.008 cm^2 area) in 180 seconds (retina radiant exposure of 4212 $J \cdot cm^{-2}$). A retinal image of 158 μm required 97.4 $W \cdot cm^{-2}$ for 180 seconds duration to produce a retinal lesion (retinal radiant exposure of 17,532 $J \cdot cm^{-2}$). Thus, as the size of the retinal image decreased, the retinal radiant exposure required to produce a retinal lesion increased. The 158 μm lesion required 4 times the retinal radiant exposure to produce a threshold lesion as the 1000 μm retinal image exposure.

The experimental research variables on retinal lesions include pupil size, spectral transmittance of the ocular media, spectral absorption of the retina and choroid, the criteria used to evaluate the exposures, exposure duration wavelength or waveband of the source and the size of the retinal area exposed. As the exposure duration increases, the radiant power entering the eye to produce a retinal lesion decreases until exposure duration becomes ineffective and the lesion depends on the power density entering the eye. The retinal lesion data of this study cannot be validly compared to the data of Ham et al. because the experimental apparatus was not designed for retinal lesion research, the exposure durations differed by a factor of at least 7, the animal species differed, and the exposures were suprathreshold. Ham has also showed a threshold radiant exposure of 6.91×10^4 $J \cdot cm^{-2}$ for a 1000 s exposure to the primate from IR in the 700 nm to 1400 nm wavelength range. The data of Ham et al. should be considered whenever safety criteria are formulated for retinal protection against IR.

In the early days, ocular protection was an empirical exercise in using protective devices of different types until it was demonstrated that the worker had been protected. The initial problem in any industrial environment is determining the spectral distribution of the undesirable source of the optical radiation. This may be a very difficult task but it allows subsequent protection philosophy to be based on valid concepts rather than becoming a hit-and-miss exercise. The government and industry now realize the importance of establishing the spectral distribution of the source and publications providing measurements of various industrial sources are beginning to appear in the literature.

Ocular protection has commonly taken the form of goggles, shields, or helmets using absorptive or reflective filters to control the undesirable optical radiation. Filters that absorb IR are manufactured by incorporating oxides of iron into the glass meld. For example, Crookes glass absorbs about 95% of the IR and 100% of the UV radiation. Absorptive filters absorb the undesirable radiation and transmit the visible spectrum necessary for vision. The use of absorptive filters to control IR may be a questionable concept because the absorbed radiation raises the temperature of the filter and the filter then becomes a secondary source for the re-radiation of heat directly into the eye. Protective transmittance filters have been standardized into shade numbers with specific shade numbers recommended for specific industrial tasks (45, 46).

Reflective filters are usually metallic coatings applied to the front surface of the filters and provide protection by reflecting the undesirable optical spectrum while transmitting the visible spectrum to allow one to see the task. Reflective filters are the most desirable method for ocular protection against IR because there is not heat build-up of the filter. Reflective filters can be very effective when properly chosen; for example, a gold coating reflects 96% of the IR and transmits maximally the part of the visible spectrum that is most efficient in providing vision. Platinum,

aluminum, and inconel (a mixture of iron, nickel and chromium) are other metals which provide excellent IR reflectance. The major difficulty in using reflective metallic coatings is their susceptibility to scratching, abrasions, and other "breakdowns" of the coating. This problem has been overcome by depositing hard protective coatings over the metallic film or by sandwiching the reflective coating between two layers of optical material. The second layer, that is the layer next to the eye, could then be made absorptive to control other unwanted optical radiations such as UV radiation. An example of an excellent combination protective filter was the Pfund's glass developed by American Optical Company. It consisted of a thin gold layer placed between a layer of Crookes A glass and clear crown ophthalmic glass. The clear ophthalmic crown glass provided protection for the metallic coating. The gold layer reflects 96% of the IR while it allows 75% of the visible radiation peaked at 550 nm to be transmitted. The Crookes A glass absorbs 100% of the UV radiation. The major advantage of metallic reflective coatings, in addition to their control of IR is that the lens is cooler and more acceptable to the wearer.

It may appear that the recommendation to use metallic coatings to control IR reaching the eye is "over-protection" since the data in this study clearly shows that a substantial IR exposure is needed to produce acute ocular injury. Metallic coatings provide a measure of protection against the low level chronic IR exposures typically encountered in glass and steel injuries, and serve to reduce the total heat load reaching the eye. In addition, the long term effects of acute exposure, such as those given during this study, are not known and maximum protection should be provided until the effects are more fully documented.

The American Conference of Governmental Industrial Hygienists (ACGIH) has recently published notice of intent to establish threshold limit values for the near IR in the 770 nm to 1400 nm wavelength range (47). The recommended IR exposure for wavelengths above 770 nm was 10 $mW \cdot cm^{-2}$. The data in this study indicate that the 10 $mW \cdot cm^{-2}$ figure is conservative and could be increased. We recognized that ACGIH recommendations are intended for delayed effects of chronic exposure while the data of this study concern from acute exposures; however, we are certain that our exposures were only to IR while recent measurements of rolling mills, glass furnaces, etc., indicate that a much higher proportion of UV may be contained in these relatively low temperature sources than previously suspected (42, 43). It has been shown that UV radiation in the 295 nm - 320 nm range is most efficient in producing lenticular opacities (39). In fact, the 295 nm waveband with a threshold radiant exposure of 0.15 $J \cdot cm^{2}$ is 8.3×10^{3} more effective in producing lenticular opacities than the 1250 $J \cdot cm^{-2}$ threshold for IR. Permanent lenticular opacities could not be produced with the IR exposures but were easily achieved with UV radiation. For these reasons, it is felt that the 10 $mW \cdot cm^{-2}$ recommended exposure limit for IR should be re-evaluated and increased to the more appropriate value of 25 $mW \cdot cm^{-2}$.

SUMMARY AND CONCLUSIONS

A 5000 watt Xenon high-pressure lamp was used to expose 100 pigmented rabbit eyes and 10 primate eyes to IR in the 700 nm to 1400 nm wavelength range and to the full spectrum output of the source. The ocular exposures were evaluated independently with the biomicroscope by two researchers and classified. The following findings and conclusions were drawn:

1. The primary ocular lesions resulting from exposure to IR were corneal, iris, and lenticular. Corneal damage varied from epithelial haze to erosion and usually healed within 24 hours. No endothelial damage was found. The iris showed stromal haze and swelling in the region of exposure with severe damage resulting in fibrinous inflammatory byproducts. Lenticular opacities appeared as small white dots that occurred at the level of the anterior epithelium just beneath the anterior capsule. No lenticular opacities could be induced by direct exposure to the lens nor was it possible to produce permanent lenticular damage. All lens damage depended on iris involvement.

2. Ocular damage from IR was related to the rate of delivery of the IR (Figure 10). The data indicate that as the irradiance level increases, the radiant exposure threshold decreases. Irradiance at and below 3.9 $W \cdot cm^{-2}$ resulted in threshold radiant exposures of 5500 $J \cdot cm^{-2}$ for the cornea, 3500 $J \cdot cm^{-2}$ for the iris, and 4000 $J \cdot cm^{-2}$ for the lens. If the irradiance exceeded 4.0 $W \cdot cm^{-2}$, the threshold radiant exposure was 1250 $J \cdot cm^{-2}$ for the cornea, 1250 $J \cdot cm^{-2}$ for the iris, and 2250 $J \cdot cm^{-2}$ for the lens.

3. A plot of the threshold radiant exposure versus the duration of exposure indicates that the IR ocular damage was a single process and all evidence (Figure 18) points toward heat as that process.

4. Exposures for the full optical spectrum, which included the visible and the UV spectra in the optical beam, were found to be additive for irradiance levels at 4 $W \cdot cm^{-2}$ and above. The threshold radiant exposures of 750 $J \cdot cm^{-2}$ for the cornea, 1000 $J \cdot cm^{-2}$ for the iris, and 2000 $J \cdot cm^{-2}$ for the lens were essentially identical to the IR exposure thresholds for the same irradiance levels.

5. The primate threshold radiant exposure was a factor of 6 above the respective rabbit thresholds. With irradiance levels above 4 $W \cdot cm^{-2}$, the radiant exposure thresholds for the primate were 8000 $J \cdot cm^{-2}$ for the cornea, 8000 $J \cdot cm^{-2}$ for the iris, and 10,000 $J \cdot cm^{-2}$ for the lens.

6. The recommended method for ocular protection against IR exposure was reflective metallic coatings to control the IR and absorptive filters to control other undesirable optical radiations. The metallic coating

should be the initial surface to intercept the optical beam and prevent heating of the protective lens.

7. Research on the ocular effects of IR from acute exposure is needed to produce more detailed information on the dependence of the rate of delivery of cataractogenesis. In addition, daily long-term low level exposure should be performed.

REFERENCES

1. Turner, H.S. The interaction of infrared radiation with the eye: A review of the literature. Aviation Medicine Research Laboratory, Ohio State University, 1-80, 1970.

2. Duke-Elder, Sir Stewart. Non-Mechanical Injuries. (Vol. XIV, Part II) Chapter on Radiational Injuries, 837-1004, Henry Kimpton, London, 1972 and Textbook of Ophthalmology, Vol. VI, Injuries, Henry Kimpton, London, 1954.

3. Moss, C.E., R. J. Ellis, W.E. Murray and W.H. Parr. Infrared radiation, in Manual on Health Aspects of Exposure to Nonionizing Radiation. World Health Organization, Regional Office, Copenhagen, Denmark, 1979.

4. Wiesinger, H., F.H. Schmidt, R.C. Williams, C.O. Tiller, R.S. Ruffin, D. Guerry III, and W.T. Ham, Jr. The transmission of light through the ocular media of the rabbit eye. Am. J. Ophth. 42:907-910, 1956.

5. Geeraets, W.J., R.C. Williams, C. Chen, W.T. Ham, Jr., D. Guerry III, and F.H. Schmidt. The loss of light energy in retina and choroid. Arch. Ophth. 64:606-615, 1960.

6. Boettner, E.A. and J.R. Wolter. Transmission of the ocular media. Invest. Ophth. 1:776-783, 1962.

7. Prince, J.H. Spectral absorption of the retina and choroid from 340-1700 nm. Publ. 14, Institute for Research in Vision, Ohio State University, 1962.

8. Geeraets, W.J. and E.R. Berry. Ocular spectral characteristics as related to hazards from lasers and other light sources. Am. J. Ophth. 66:15-20, 1968.

9. Verhoeff, F.H. and L. Bell. The pathological effects of radiant energy on the eye. Proc. Am. Acad. Arts Sci. 51:627-818, 1915-16.

10. Dawson, W.W. Experimental ocular pathology related to corneal transmittance and infrared psychophysics. J. Appl. Phys. 18:1013-1016, 1963.

11. Meyenhofer, W. Zur Aetiologie des graven Staars: Jugendliche Katarakten bei Glasmachern. Klin. Monatsbl. Augenh. 24:49-67, 1886.

12. Legge. Home Office Report on Glassworkers, London, 1907, cited in Parsons, J.H. Some effects of bright light upon the eyes. J.A.M.A. 55:2027, 1910.

13. Legge. Ophthal. Rev. 33, 28-30, 1914.

14. Robinson, W.D. Glassblower's cataract. Ophthalmologica. 13:538-554, 1915.

15. Vogt, A. Einige Messungen der Diathermansie des menschlichen Augapfels und seiner Medien, sowre des menschlichen Oberlides, nebst Bemerkungen zur biologischen Wirkung des Ultrarot. Arch. f. Ophth. 83:99-1131, 1912.

16. Vogt, A. Fundamental investigations of the biology of infrared. Klin. Monatsbl. Augenheilk. 89:256-258, 1932.

17. Goldmann, H. Kritische und Experimentelle Untersuchungen uber den Sogenannten Ultrarotstar der Kaninchen und der Feverstar. Arch. f. Ophth. 125:313-402, 1930.

18. Goldmann, H. Experimentelle Untersuchungen uber due Genese des Feverstarres; uber Arbeitshyperthermie bei Feverarbeitern. Arch. f. Ophth. 128:648-653, 1932.

19. Goldmann, H. Genesis of heat cataract. Arch. Ophth. 9:314, 1933.

20. Goldmann, H. Experimentelle Untersuchungen uber die Genese des Feverstars, I Teil. Arch. f. Ophth. 130:93-130, 1933.

21. Goldmann, H. Experimentelle Untersuchungen uber des Feverstares: die Physik des Feverstars, II Teil. Arch. f. Ophth. 130:131-139, 1933.

22. Goldmann, H. Experimentelle Untersuchungen uber die Genese des Feverstares: die Physik des Feverstars, III Teil. Arch. f. Ophth. 130:140-179, 1933.

23. Goldmann, H. The genesis of the cataract of the glass blower. Ann. Ocul. 172:13, 1935, Am. J. Ophth. 18:590, 1935.

24. Goldmann, H., H. Konig, and F. Mader. Die Durchlassigkeit der Augenlinse fur Infrarot. Ophthalmologica. 120:198-205, 1950.

25. Kutscher, C.F. Ocular effects of radiant energy. Ind. Med. 15:311-316, 1946. Trans. Amer. Acad. Ophthal. and Otolyog., Vol. 50, 230-241, 1946.

26. Salit, P.W. Sex incidence of cataract with special reference to its exogenous causes. Acta Ophth. 18:309-320, 1940.

27. Dunn, K.L. Cataract from infra-red rays (glassworker's cataracts). AMA Arch. Ind. Hyg. Occup. Med. 1:160-180, 1950.

28. Keatinge, G.F., J. Pearson, J.P. Simons, and E.E. White. Radiation cataract in industry. Arch. Indus. Health. 11:305-314, 1955.

29. Wallace, J., P.M. Sweetman, C.G. Warner, P.A. Graham, and A.L. Cochrane. An epidemiological study of lens opacities among steelworkers. Brit. J. Indus. Med. 28:265-271, 1971.

30. Langley, R.K., C.B. Mortimer, and C. McCullough. The experimental production of cataracts by exposure to heat and light. Arch. Ophth. 63:473-488, 1960.

31. Pitts, D.G. and A.P. Cullen. Ocular ultraviolet effects from 295 nm to 335 nm in the rabbit eye. DHEW (NIOSH) Publication. No. 77-130, 1-55, 1976.

32. Bredemeyer, H.G., O.A. Wiegmann, A. Bredemeyer, and H.R. Blackwell. Radiation thresholds for chorioretinal burns. Technical Documentary Report No. AMRL-TDR-63-71, 6570th Aerospace Medical Research Laboratories, Wright-Patterson AFB, Ohio. July 1963.

33. Jacobson, J.H., B. Cooper, and H.W. Najac. Effects of thermal energy on retinal function. Technical Document Report No. AMRL-TDR-62-96, Life Support System Laboratory, Wright-Patterson AFB, Ohio. August 1962.

34. Ham, W.T. Jr., H.A. Mueller, J.J. Ruffold Jr., and A.M. Clarke. Sensitivity of the retina to radiation damage as a function of wavelength. Photochem. and Photobiol. Vol. 29, 735-743, 1979.

35. Barthelmess, G.A. and J. Borneff. Uber die Gewebliche schadigung der Augenlinse durch Warmestrahlung. Arch. f. Ophth. 160:641-652, 1959.

36. Sliney, D.H. and B.C. Freasier. Evaluation of optical radiation hazards. Applied Optics. 12:1-24, 1973.

37. Pitts, D.G. and A.P. Cullen. Ocular ultraviolet effects from 295 nm to 400 nm in the rabbit eye. DHEW (NIOSH) Publication No. 77-175, 1977.

38. Hager, G., S. Pagel, and D. Broschmann. Fire cataracts among locomotive firemen. Verk. Med. Vol. 18, 443-449, 1971.

39. Ruth, W., M. Levin, and B. Knave. Occupational hygienic evaluation of infrared emitters for drying automobile enamel. Study Report AMMF 104/76, Stockholm, 1976.

40. Edbrooke, C.M. and C. Edwards. Industrial radiation cataract: The hazards and the protective measures. Ann. Occup. Hyg. 10:293-304, 1967.

41. Cogan, D.G., D.D. Donaldson, and A.B. Reese. Clinical pathological characteristics of radiation cataract. Arch. Ophth. 47, 55-70, 1952.

42. Duke-Elder, Sir S. System of Ophthalmology, Vol. XI, Diseases of the Lens and Vitreous. Glaucoma and Hypotony. Henry Kimpton, London, p. 81, 1969.

43. Hiller, R., L. Giacometi and K. Yuen. Sunlight and cataract: An epidemiologic investigation. Am. J. Epidimol. Vol. 105, 450-459, 1977.

44. Ham, W.T., H.A. Mueller, R.C. Williams, and W.J. Geeraets. Ocular hazard from viewing the sun unprotected and through various windows and filters. Applied Optics, Vol. 12, 2122-2129, 1973.

45. U.S. Department of Labor, Code of Federal Regulations, Title 29, Chapter XVII, Part 1910.252, Welding, Cutting and Brazing, 1976.

46. American National Standards Institute, American National Standard Practice for Occupational and Educational Eye and Face Protection, ANSI Z87.1-1979, 1979.

47. American Conference of Governmental Industrial Hygienists, Threshold Limit Values for Chemical Substances and Physical Agents in the Workroom Environment with Intended Changes for 1979, 90-92, 1979.

48. Barker, F.M. III. The transmittance of the electromagnetic spectrum from 200 nm to 2500 nm through the optical tissues of the pigmented rabbit eye, Master's Thesis, University of Houston, College of Optometry, December 1979.

☆ U.S. GOVERNMENT PRINTING OFFICE: 1980-657-147/5865